Division of Biomedical Engineering, Department of Human Biology

University of Cape Town

Final dissertation for fulfillment of requirements for the degree

MSc (Med) in Biomedical Engineering

OSSEOINTEGRATION POTENTIAL FOR HEAT TREATED 3D TI6AL4V SCAFFOLDS SEEDED WITH MESENCHYMAL STEM CELLS *IN VITRO*

Investigator: Esther van Heerden (VHREST002)

Supervisor: Dr George Vicatos

Co-Supervisor: Prof Susan Kidson

March 2014

Acknowledgements

I would like to thank the following people for their help, in various aspects, in making the completion of this Masters dissertation possible:

First and foremost, I'd like to thank my fiancé Mark for his unconditional love and support, both emotionally and financially. If it weren't for you, this journey would not have been possible, from start to end.

To my family, for all their support and encouragement, and for providing me with a world of opportunities growing up, thank you.

Dr George Vicatos and Prof Susan Kidson, your guidance and support during this project have been incomparable. Thank you for giving me the opportunity to pursue this research, and in doing so, introducing me to exciting new fields of work.

Dr Robea Ballo, thank you for your tissue culture and laboratory help.

To Toni Wiggins thank you for teaching me the ropes and all your subsequent help with my cells. Your knowledge and expertise are invaluable. But most of all, thank you for the many long chats filled with much needed advice and surety.

To Gerrie Booysen and Johan Els at the Centre for Rapid Prototyping and Manufacturing at the Central University of Technology, thank you for the manufacturing of the Ti64 scaffolds, needed for my research, and for technical help.

To Dr Niel Davies at the Cardiovascular Unit at University of Cape Town, and to Marnie Potgieter from Institute for Cellular and Molecular medicine at the University of Pretoria, thank you for providing with the stem cells needed to make my research possible, and for the troubleshooting help.

To a the number of people that have helped me in the technicalities of my work, Penny at the Department of Materials Engineering for help with the etching and heat treatment of my scaffolds; Morea and Susan, both in the Department of Human Biology, for help with the staining and microscopy of my cells. Thank you all.

Finally, but by no means least, thank you to the National Research Foundation and to the Biomedical Engineering Research Group at the University of Stellenbosch for the financial support of the project.

Plagiarism Declaration

I, Esther van Heerden, hereby declare that the work done in this dissertation is my own and has not been obtained from other research. In contributions to this work, I have stated and acknowledged other research using the Harvard referencing style. I have not allowed my work to be submitted for any other qualification at University of Cape Town or any other academic establishment.

Signature:_____

Abstract

Aseptic loosening of artificial joints occurs due to the loss of implant fixation. By implementing a 3D porous structure at the bone-implant interface, the ingrowth of bone will permit better and stronger interlocking of the implant to prevent loosening. In this study, it is hypothesized that the seeding of 3D scaffolding structures with mesenchymal stem cells (MSCs) will improve the potential for osseointegration of the implants, as the existing bone may be more inclined to unite with developing bone than with the implant substrate. Titanium-6 Aluminium-4 Vanadium (Ti64) is one of the most commonly used implant materials. Heat treatment of Ti64 was seen in tests done at the University of Cape Town to further improve against implant failure by vastly improving the materials strength and reducing debris formation. Thus the aim of this study was to investigate the effects the heat treatment of Ti64 would have on the capabilities of seeded MSCs *in vitro*.

Ti64 scaffold disks were manufactured and heat treated at 600 °C for 20 hours to obtain thermal oxidisation. All cell tests were done with rat and human MSCs. Seeding efficiency tests were done to measure the number of cells that adhered to the Ti64 substrates over a 24 hour period. Rat MSCs appeared to adhere slightly more to the untreated Ti64, and human to the heat treated Ti64, but results were near comparable. Growth of MSCs on the Ti64 substrates was measured over a 21 day period. Both the rat and human MSCs appeared to grow marginally slower on the heat treated Ti64, but not considerably so. Finally, the differentiation of MSCs were measured and observed on the Ti64 substrates over a 26 day period. Rat MSCs appeared to differentiate slightly less, whereas human MSCs slightly more on the heat treated Ti64. Again, the results did not notably differ between the substrates. These results indicate that the heat treatment of Ti64 did not adversely affect the MSCs capabilities. This suggests identical therapies may be implemented on the heat treated Ti64 as on the untreated. Unexpected results from this study showed that the cells location within the scaffold (i.e. on the base versus on the struts), as well as the cells age, albeit the patients age or the length of time in culture, appeared to notable affect the cells capabilities on the Ti64 substrates.

Table of Contents

List of Figures

List of Tables

List of Abbreviations

3D	Three dimensional
°C	Degrees Celsius
αMEM	Alpha Minimum essentials medium
ALP	Alkaline Phosphatase
CAD	Computer Aided Design
CD	Cluster of differentiation
cm^2	Squared centimetre
Cells/cm^2	Cells per squared centimetre
CRPM	Centre for Rapid Prototype Manufacturing (at CUT)
CUT	Central University of Technology (Bloemfontein)
DMEM	Dulbecco's modified Eagles medium
DMSO	Dimethyl sulfoxide
EDTA	Ethylenediaminetetraacetic/Edetic acid
FBS	Foetal Bovine serum
g	Grams
hFibs	Human fibroblasts
hMSCs	Human MSCs
kPa	Kilopascal
m	Metre
mg	Milligram
ml	Millilitre
MSCs	Mesenchymal stem cells
nm	Nanometre
rMSCs	Rat MSCs
RPD	Rapid Prototype Development
SLS	Selective Laser Sintering
Ti64 / Ti6Al4V	Titanium – 6 Aluminium – 4 Vanadium
UCT	University of Cape Town
µg	Microgram
µl	Microlitre
µm	Micrometre
U/ml	Units per millilitre

1 Statement of the Problem

Joint replacement surgeries, or arthroplasties, are becoming more frequent around the world as lifestyle habits change and life expectancy increases due to improved health care. Arthritis is one of the leading causes for arthroplasty procedures; however, the rate at which a joint will deteriorate will depend on patient factors such as their age and gender, weight and activity levels. A weight bearing joint such as a hip or knee will undergo much higher strains than that of a non-weight bearing joint and is thus more likely to need replacement. Analysis of arthroplasty trends in 2005 shows a projected 174% increase in total hip arthroplasties and 673% increase in total knee arthroplasties by the year 2030 in the United States (Kurtz, Ong, Lau, Mowat, & Halpern, 2007). Data collected for England and Wales show an increase of 17.5% of arthroplastic surgeries between 2007 and 2012 (National Joint Registry, 2012).

Due to the advancements in healthcare, people are living longer resulting in a problem that patients are beginning to outlive the designated life of their artificial joints. This problem has led to the prevalence of a second revision surgery on the artificial joint. Revision surgery is done to replace and/or correct an existing artificial joint. Failure of the initial artificial joint may be due to various reasons, however the National Joint Registry report (2012) states that the most frequent reason for revision surgery is due to aseptic loosening of the joint, followed by cases of dislocation. Aseptic loosening of the joint occurs through the loss of implant fixation to the bone for various reasons, resulting in joint movement and instability. According to Kurtz *et al*. (2007) it is expected that by 2025 the number of hip arthroplasty revisions will double that of 2005, and knee arthroplasty revisions will double by 2015, illustrating the severity of this problem.

From previous work done by various authors, one can determine a number of key points to be considered in implant development for the combating of aseptic loosening:

- Ti64 is biocompatible with osseointegrating capabilities (Dabrowski, Swieszkowski, Godlinski, & Kurzydlowski, 2010; Li *et al*., 2007; Palmquist *et al*., 2009; Steinemann, 1998)
- Thermal oxidisation reduces contributing mechanical debris, as well as improving mechanical characteristics of Ti64 (Allen, Bloycet, & Bell, 1996; Mudd, Vicatos, & Basson, 2003)
- 3D surface, or structure on the surface, of an implant allows for bone ingrowth and thus a stronger implant attachment (Engler, Sen, Sweeney, & Discher, 2006; Le Guehennec *et al*., 2008; Le Guehennec, Soueidan, Layrolle, & Amouriq, 2007; Li *et al*., 2007)
- Cells seeded on Ti64 will adhere, proliferate and differentiate (Baba *et al*., 2010; Lavenus *et al*., 2011; Maeda, Hirose, Ohgushi, & Kirita, 2007; Perrotti *et al*., 2013; Stiehler *et al*., 2008; St-Pierre, Gauthier, Lefebvre, & Tabrizian, 2005)

In this study, it is hypothesised that the seeding of three dimensional structures with cells that are able to differentiate and produce bone will improve the potential for osseointegration of the implants. However, from these key points arises another important issue which will subsequently be investigated in this study:

- The effect that heat treatment of Ti64 will have on seeded cell capabilities such as seeding, proliferation and differentiation.

The following components, although not the main focus, play a vital role in the success of this investigation into the heat treatment effects and would thus need to be accomplished in order to fulfil the main objective of this study:

- Develop a 3D structure on the surface of an implant manufactured from heat treated Titanium-6Aluminium-4Vandaium (Ti64) to provide a 3D scaffold for bone ingrowth and attachment

- Seed these scaffolds with mesenchymal stem cells (MSCs) to differentiate into osteoblasts in order to further improve the osseointegration of the implants

1.1 Scope and Limitations

To assess the effects of heat treatment on the osseointegration potential of Ti64 the study will perform *in vitro* assessments of the untreated and heat treated three dimensional (3D) Ti64 scaffolds seeded with mesenchymal stem cells. This study will not test any *in vivo* conditions for the seeded heat treated Ti64 scaffolds. The Ti64 scaffolds will be seeded using rat and human mesenchymal stem cells respectively. The rat MSCs will be used in preliminary proof of principal tests, followed by the testing of human MSCs to ascertain cell performance for possible future application. The Ti64 scaffolds will be manufactured through the process of laser sintering; other development processes have not been considered.

1.2 Plan of development

This report will begin with an intensive literature review in chapter 2, where the biological and engineering concepts will be analysed separately before linking them and identifying where the gaps in knowledge lie. From this, chapter 3 will clarify and define the aims and objectives specific to this study. Experimental methods will be set out in chapter 4 prior to the presentation of the experimental results in chapter 5. The results illustrated in chapter 5 will then be discussed further and analysed in more depth in chapter 6 enabling conclusions to be drawn in chapter 7 and finally recommendations for future work to be drawn up in chapter 8.

2 Literature Review

Aseptic loosening is defined as the loosening of an implant. It may be a result of poor initial fixation, mechanical loss of fixation or biological loss of fixation. The biological loss of fixation is due to the generation and release of tiny particles of debris from the implant articulation surface. This problem can be attributed to the poor tribology of the implant material. Tribology is the study of articulating surfaces with regards to friction, lubrication, wear and debris. When the prosthesis has been implanted and is subjected to long term stressful conditions such as weight bearing stresses and as the continued sliding against another implant component occurs, the surface of the material may begin to delaminate and erode. This fretting process results in the production of these wear debris particles which act as third body abrasives at the sliding interface and when expelled into the immediate surrounds (Allen *et al*., 1996; Díaz *et al*., 2008).

The presence of debris in the surrounding tissues will generate a chronic inflammatory response, whereby the site of debris would be invaded by macrophages and multinucleated giant cells (Anderson, 2001; Brodbeck & Anderson, 2009; Haleem-Smith *et al*., 2012). These cells are commonly found at biomaterial implants as they are able to digest foreign particles through phagocytosis to clear the area of debris particles. When the amount of debris produced from the articulating surfacing escalates and overpowers the cells ability to digest and discard it, the particles will remain as an abrasive between the articulating surfaces and will accumulate in the surrounding tissues. This will lead to the mechanical deterioration of the joint, reduced cell viability, proliferation and differentiation, as well as increased osteolysis resulting in joint loosening (Allen *et al*., 1996; Anderson, 2001; Brodbeck & Anderson, 2009; Haleem-Smith *et al*., 2012). In most cases, the debris particles are only apparent at later stages of aseptic loosening once the revision surgery is already required (Abu-Amer, Darwech, & Clohisy, 2007).

The challenge of overcoming aseptic loosening has two very distinct components of equal importance that would need to be considered; the implant itself and the biology of the tissue into which it is implanted. This chapter will initially introduce biomaterials used for implant in section 2.1, followed by an overview of the biology of bone in section 2.2. Having the basis of both separate components, section 2.3 will then talk about the development of implants and section 2.4 will combine all these aspects, showing how they interact together, and how this will be translated into objectives of this project.

2.1 Biocompatible materials

The use of various biomaterials to restore or replace degenerated connective tissue is widely practiced in the medical field, and has extensively reduced pain and improved patient's quality of life (Oreffo & Triffitt, 1999). Metals have successfully been in use as implant materials since 1895 when Lane first used steel as a fracture fixation plate (Lane, 1895). Tests, however, were done as early as 1829, when Levert began experimenting with implanting gold, silver, lead and platinum specimens into dogs to observe their effects (see Ratner, Hoffman, Schoen, & Lemons, 2012). After its development in the 1920's, stainless steel's superior corrosion resistance made it a mainstream biomaterial in the medical industry (Hermawan, Ramdan, & Djuansjah, 2009). By the end of the 1920's, vitallium, a cobolt-chromium-molybdenum (Co-Cr-Mo) alloy still popular today, was developed and successfully used as an implant with superior strength. The initial use of polymers, nylons and other synthetic materials for implantation began in the 1940's. These synthetic materials were mainly used for suturing purposes as adverse reactions were seen when implanted possibly from polymer leaching. That was until around the 1960's when research into these materials advanced and they were able to specifically develop them for biomedical use (Ratner *et al*., 2012). The idea of using titanium (Ti) as an implant material was initially suggest by Cotton in 1947; it was only in 1952 that its true osseointegration potential was discovered when Brånemark tried to remove a titanium screw from a rabbit bone at the end of

a several month long experiment and found it deeply embedded in the bone (Ratner *et al*., 2012).

Commercially pure Ti has shown excellent osseointegration capabilities, such as in Brånemark's work above, but it lacks the mechanical strength required to replace or repair bone (Anchorage, 1981; Ratner *et al*., 2012; Steinemann, 1998). Ti alloy, particularly Titanium-6Aluminum-4Vandium (Ti64) has since become a widely used implant in orthopaedic and maxillofacial and oral surgery due to its improved strength (Steinemann, 1998; Dabrowski, *et al*., 2010; Li, *et al*., 2007). Although Ti64 has proved itself mechanically, there has long been doubt that it, or any other Ti alloy, is able to osseointegrate as well as commercially pure Ti (Anchorage, 1981; Steinemann, 1998). Palmquist *et al*. (2009) has however recently shown that when Ti64 is machined to present a surface structure comparable to that of commercially pure Ti, the adherence of bone to the alloy is identical to that of the commercially pure Ti. This shows that by using Ti alloys, one is able to obtain mechanical strength while maintaining osseointegration abilities.

Each quality that adds to Ti64 being the most commonly used implant material will be spoken of in more depth in the following subchapters. Section 2.1.1 will talk about the Ti's oxide film that forms and contributes to the biocompatibility of the metal, and section 2.1.2 will explain Ti64's microstructure and how this mechanically contributes to the implant. Section 2.1.3 will then lay out how the use of heat treatment processes may alter these qualities.

2.1.1 Ti oxide film and biocompatibility

Titanium is known as a biocompatible metal as it shows no adverse or allergic reactions when implanted in the body (Steinemann, 1998). Ti is a reactive metal, in that it undergoes a reaction with oxygen molecules from its surrounding environment (water, air, extracellular matrix); but in doing so, it instantly creates an electrically and chemically inert film of titanium oxide (TiO_2) of approximately 4 nm thick on the surface of the metal (Schindler, 1984). This film formation is unique to

Ti metals and occurs by the diffusion of oxygen ions between the Ti molecules and into the metals surface, shown in Figure 2.1 A. The exposed oxygen molecules are hydroxylated in the presence of water molecules (water, air moisture or tissue fluids) as seen in Figure 2.1 B, thus resulting in no Ti ion being present at the surface and in contact with the surrounding environment (Steinemann, 1998). With respect to implants, this film is an important barrier preventing contact with and loss of metal ions into surrounding tissues and consequently avoiding any adverse reactions (Steinemann, 1998).

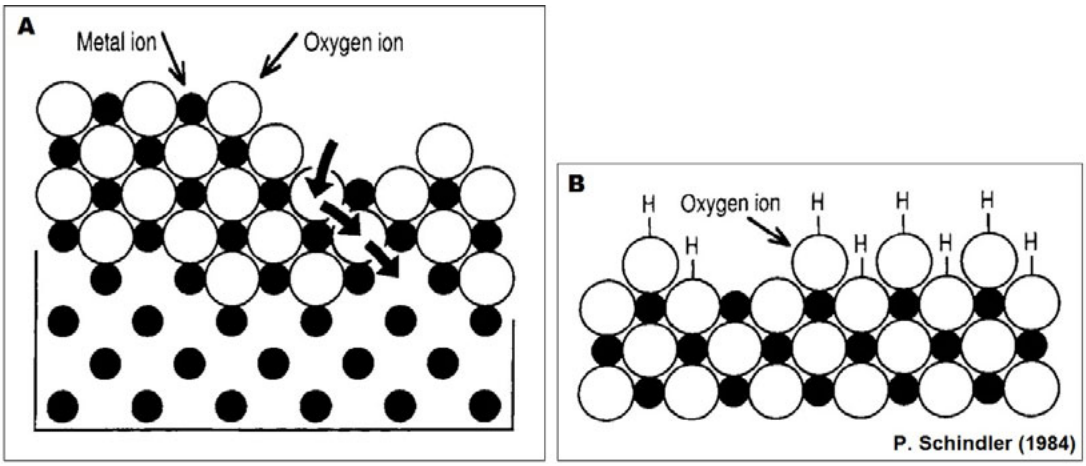

Figure 2.1 Formation of TiO_2 film. (A) Migration of oxygen molecules into titanium surface, (B) hydroxylation of surface oxygen molecules (Steinemann, 1998)

2.1.2 Ti64 microstructure and mechanical compatibility

Commercially pure Ti is not mechanically strong enough to replace bone as mentioned previously but it is possible to alter its microstructure in order to obtain the mechanical strength desired. This is possible due to the allotropic crystal structure of Ti, meaning its ability to reversibly change its crystal structure. When the metal reaches a temperature of around 880 °C, its crystal structure will change from alpha (α) phase (hexagonally close packed) to a beta (β) phase (body centred cubic)(Pederson, 2002; Pohler, 2000).

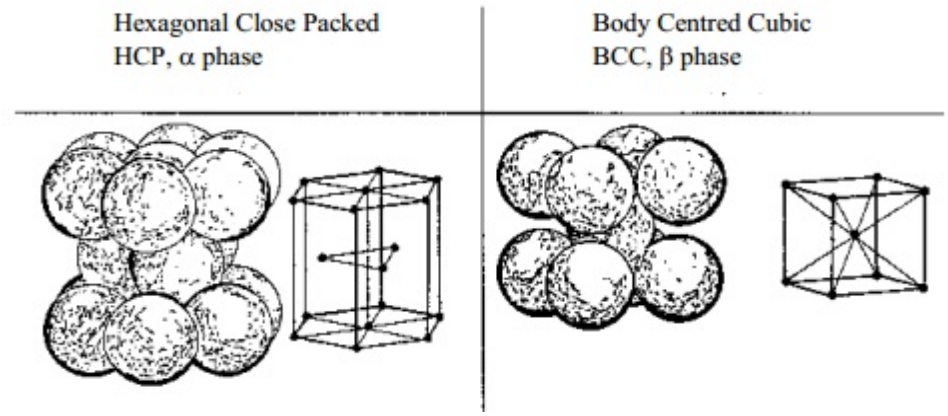

Figure 2.2 Crystal structures of alpha and beta phase titanium (Pederson, 2002)

Both α and β phases (shown in Figure 2.2) have advantages; Ti in α phase has increased tensile strength, creep strength and higher elastic modulus whereas Ti in β phase is more ductile. In order to produce a suitable implant, it must include qualities from both α and β phases of Ti. The implant will need high tensile strength associated with α phase to withstand high impact and excessive loads that weight bearing bones and joints are exposed to, as well as ductility associated with β phase to be able to deform and not fracture (usually due to fatigue) when withstanding cyclic loading. (Frosch & Stürmer, 2006; Pederson, 2002; Pohler, 2000)

This combination is achieved by alloying Ti with other elements to obtain an ideal balance of alpha-beta (α-β) phase at room temperature. Alpha stabilizers such as aluminium (Al), oxygen (O), and nitrogen (N), are elements that raise the transus temperature at which the α phase structure changes to β phase shown in Figure 2.3 A.

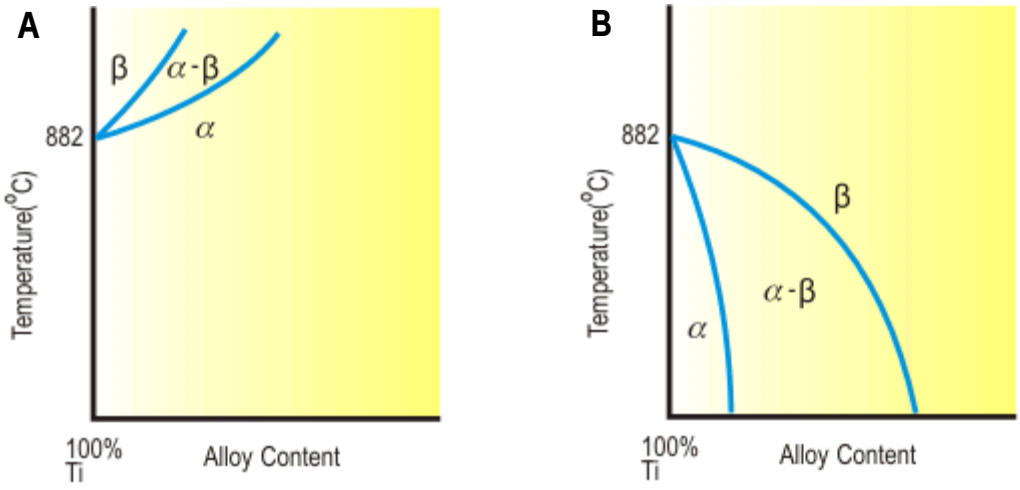

Figure 2.3 (A) Effects of alpha stabilisers on transient temperature (AZOM.com), (B) Effects of beta stabilisers on transient temperature (Azom.com)

Beta stabilizers such as vanadium (V), iron (Fe), niobium (Nb), are elements that will lower the transus temperature at which the β phase structure changes to α phase shown in Figure 2.3 B. The addition of α and β stabilizers to commercially pure Ti will result in a α-β region (seen in Figure 2.3 A and B) in which characteristics of both phases will be seen in the metal (Frosch & Stürmer, 2006; Pohler, 2000; Steinemann, 1998).

Elements used as α and β stabilizers will determine the final degree of allotropy of the metal. By using aluminium and vanadium as alloying elements, Ti64 remains biocompatible and falls into the desired α-β alloy category at room temperature with the required mechanical characteristics. The use of vanadium in biomaterials has had mixed reviews in the past due to its cytotoxicity and possible leaching into surrounding tissues. Bracken, Sharma, & Elsner's (1985) work showed the morphological changes in bovine kidney cells due to the uptake of vanadium. Waters, Gardner, & Coffin (1974) showed that reduced viability and total number of rabbit alveolar macrophages after exposure to various forms of vanadium. In individuals that do have a cytotoxic reaction to Vanadium, Niobium is often used to replace it in the alloy. Perren, Geret, Tepic, & Rahn (1986) on the other hand

showed, by quantifying the effects on individual cells during *in vivo* animal tests, that although the vanadium element has a cytotoxic response, vanadium containing alloys has similar biological compatibility as Vanadium-free alloys, including Ti6Al7Nb.

2.1.3 Thermal oxidisation

Thermal oxidization is a heat treatment process which commercially pure or alloyed Ti can be subjected to in order to alter the crystal structure and increase the depth of the oxide layer. The crystal structure of the oxide layer is altered during thermal oxidization to express more α phase Ti structure but without losing β phase qualities. This structural change provides a much greater surface hardness, elastic modulus and wear resistance to the material, thereby further reducing the risk of failure of the implant (Allen *et al*., 1996; Díaz *et al*., 2008; Guleryuz & Cimenoglu, 2005; Waterhouse & Iwabuchi, 1985).

A unique process of thermal oxidisation, or heat treatment of Ti64 has been developed at the University of Cape Town (UCT). Allen *et al*. (1996) shows that by extending the heat treatment time, one is able to increase the oxide layer depth up to approximately 20 µm. Further work done at UCT by Mudd *et al*. (2003) tested the treatment capabilities via loaded sliding wear tests which is done by simulating the sliding of a knee joint of a person, in this case a 90 kg person. When Ti64 was subjected to a heat treatment of 600 °C for 20 hours, zero wear or debris production was seen after approximately 53,000 m of sliding, or 2,000,000 cycles. A clearly define “diffusion zone” was also seen showing the extent of the oxide layer. Mudd *et al*. (2003) also tested the heat treatment at a temperature of 700 °C for 10 hours which resulted in large segments of the oxide layer shearing off during a relatively short sliding distance of less than 5,000 m. No “diffusion zone” was seen in the 700 °C heat treated sample. Although the newly exposed Ti64 will reoxidise in contact with the extracellular fluids, it is the large sheared off segments of oxide layer that will act as a third particle abrasive and tissue irritant and enable the continued deterioration. This shows that there is an optimal heat treatment

temperature for the oxygen to diffuse into the surface to harden and strengthen the immediate substrate and thus form a defined interlayer.

2.2 Bone Development

Bone is a specialised type of connective tissue that forms the structural scaffolding of the body and the attachment points for muscles. It is comprised of water, hydroxyapatite [$Ca_{10}(PO_4)_6(OH)_2$] crystals with traces of other ions and 25% organic compounds such as type 1 collagen and noncollagenous proteins (Kerr, 2010; Ross & Pawlina, 2011). This chapter will introduce the different cells types found in bone and the processes of bone formation. Finally, the mechanisms of bone remodelling and repair for the maintenance of bone will be described.

2.2.1 Types of bone

In a developing foetus, or in fracture repair where there is rapid bone remodelling occurring, immature bone is formed in random patterns and is often referred to as woven bone due to irregular arrangement of collagen fibres. More cells are present in immature bone, randomly placed, for the fast production of the bone matrix. As time progresses, woven bone is gradually replaced with mature organised bone, known as mature or lamellar bone. Mature bone consists of two types, compact bone and spongy bone.

The first type of mature bone is compact or cortical bone which is found in the shaft of long bones and the surface of flat bones. It is largely comprised of cylindrical osteons made up of lamella of densely packed collagen fibres and bone matrix as seen in Figure 2.4. Osteons will generally lie parallel to the long axis of the bone and may end blindly or branch off into multiple osteons. At the centre of each osteon is a Haversian canal in which the neurovascular supply for the osteon runs. The Haversian canals of neighbouring osteons are connected via perpendicular Volkmann's canals to link the neurovascular supply (Kerr, 2010; Kierszenbaum, 2007; Ross & Pawlina, 2011).

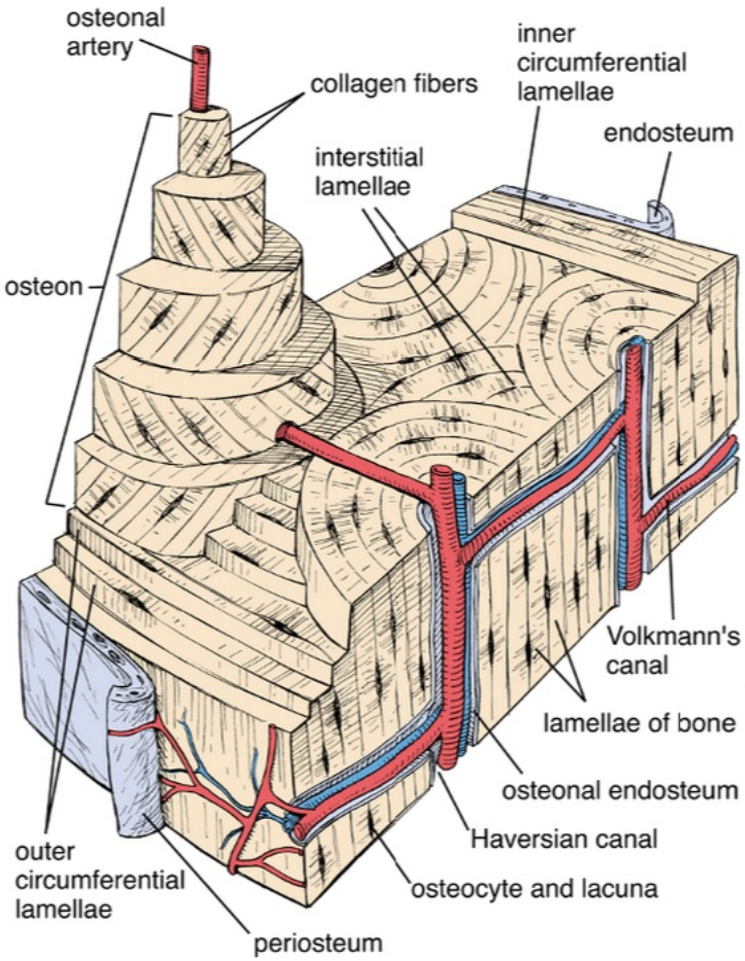

Figure 2.4 Section of compact bone showing Haversian system (Ross & Pawlina, 2011)

The second type of mature bone is spongy or trabecular bone which is found at the ends of long bones and the centre of flat bones. Spongy bone is micro-structurally similar to compact bone but does not have the regularity of compact bone. Rather than the concentric layout of osteons, the lamellar in spongy bone has a parallel pattern and is arranged into connecting struts or trabeculae. This structuring results in a very light and porous bone in which most of its volume may be filled with bone marrow as seen in Figure 2.5 (Kerr, 2010; Kierszenbaum, 2007; Ross & Pawlina, 2011).

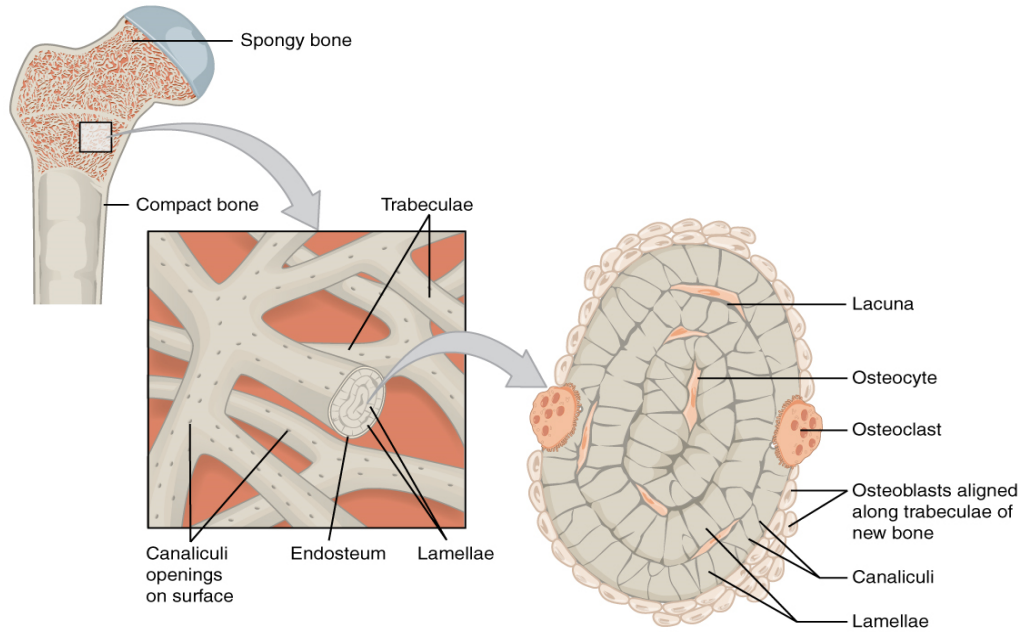

Figure 2.5 Section of spongy bone showing trabeculae detail (cnx.org/content/m47981)

2.2.2 Bone cells

There are five types of cells present in bone tissue that are associated with the development and maintenance of bone (refer to Figure 2.6):

1. Mesenchymal stem cells (MSCs)

Mesenchymal stem cells (MSCs) are a multipotent naïve cell derived from the mesoderm layer of a forming embryo. These cells are defined by their by their ability to adhere to plastic when in culture; their ability to differentiate and form various mesenchymal tissues such as bone, muscle, cartilage, marrow, tendon, ligament and fat; as well as their expression of certain cluster of differentiation (CD) surface markers. CD markers are important in guiding the direction of differentiation. Due to their multipotency, they may be found in stem cell niches all over the body and in various tissues ready to differentiate (Okochi, 2011; Zhao, 2013).

When considering bone tissue, mesenchymal stem cells are the precursor for three of the four other bone cells. Runx2 is a transcriptional protein factor that will

induce the differentiation of these cells into osteoprogenitor cells and later into osteoblasts, and is regulated by bone morphogenic proteins. These cells are found in continuous supply within the bone's marrow and in the surrounding periosteum for bone development (Karsenty, 2007; Komori, 2006).

2. Osteoprogenitor cells

Osteoprogenitor cells are osteoblast precursor cells that are derived from MSCs. These cells still have stem cell like qualities, as they are still able to proliferate and differentiate. Differentiation of these cells is activated during growth and during fracture repair when the transcriptional factor osterix has been triggered. Osteoprogenitor cells are quiescent when not activated in the growth or repair of bone, and are known as bone lining cells as they are located along the bone surfaces in the periosteum and endosteum. (Kerr, 2010; Kierszenbaum, 2007; Komori, 2006; Ross & Pawlina, 2011)

3. Osteoblasts

Osteoblasts are osteocyte precursor cells and are derived from osteoprogenitor cells. Runx2 that was activated in MSCs to induce differentiation into osteogenic cells is now turned off as osteoblasts mature and change from proliferating and differentiating cells to secretory cells that are responsible for the mineralization of bone matrix. The presence of osterix will now induce the osteoblasts secretion of osteoid, which is the organic portion of bone matrix made up of calcium-binding proteins, glycoproteins, proteoglycans and alkaline phosphatase (ALP) enzymes. ALP enzymes are able to hydrolyse secreted inorganic pyrophosphate to produce free phosphate ions. These phosphate ions will complete the hydroxyapatite crystals (Kerr, 2010; Kierszenbaum, 2007; Orimo, 2010; Ross & Pawlina, 2011).

4. Osteocytes

Osteocytes are osteoblasts that have been encased in mineralized osteoid. Each osteocyte occupies a space known as a lacuna. Lacunas are connected to each other through canaliculi, in which the osteocytes may extend cytoplasmic processes to communicate with one another. These cells are responsible for maintaining the surrounding bone tissue. They are able to respond to mechanical forces and synthesize new osteoid if need be, by maintaining or altering the surrounding calcium and phosphate levels. Osteocytes may remain in place for many decades, however with age and the reduction of blood supply, bones may become brittle as these regulating and maintaining cells begin to die (Kerr, 2010; Komori, 2006; Ross & Pawlina, 2011).

5. Osteoclasts

Osteoclasts are the final cell type associated with bone development and maintenance and are the only ones not of mesenchymal stem cell origin. These are large multi-nucleated cells are derived from mononuclear haemopoietic progenitor cells under the induction of c-fos and NFKB transcriptional factors. These cells are the responsible for the resorption of bone during the bone remodelling process through phagocytosis. Once the cells have resorbed the bone and formed a lacuna, the cell may either move to a new site or may undergo apoptosis (Kerr, 2010; Ross & Pawlina, 2011).

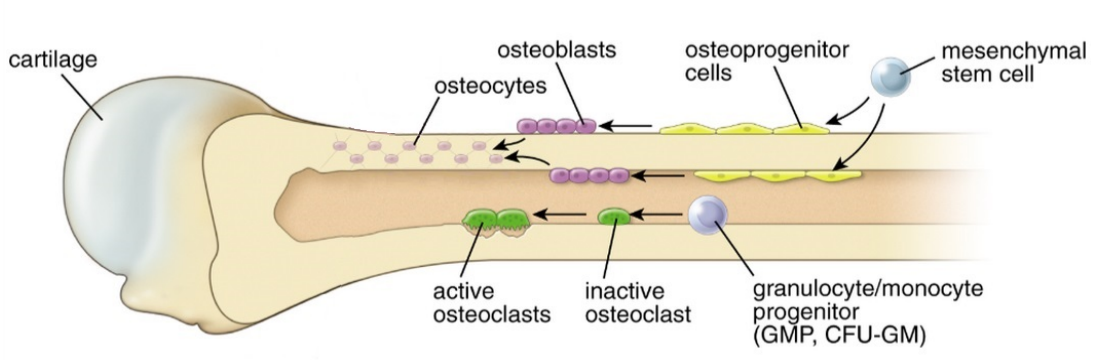

Figure 2.6 Type of cells and their location within bone (Ross & Pawlina, 2011)

2.2.3 Bone formation

Bone formation can be split into two modes of ossification, intramembranous and endochondral. Essentially the mechanisms of each mode of ossification is the same, both using the cells and processes as described in section 2.2.2; the difference being that in endochondral ossification the production of bone replaces an existing cartilage model.

2.2.3.1 Intramembranous Ossification

Intramembranous ossification occurs when bone is formed through the differentiation of mesenchymal stem cells into osteoid producing osteoblasts. As the osteoblasts become surrounded by osteoid, changing into osteocytes, surrounding mesenchymal stem cells will differentiate into osteoprogenitor cells and then osteoblasts, produce osteoid and so forth. This increase in bone size is known as appositional growth and gives rise to woven bone which will later be remodelled into lamellar bone. Flat bones such as facial and cranial bones are created this way. The diameter of long bones are able to increase by a combination of appositional growth and bone resorption as seen in Figure 2.7 (Kerr, 2010; Kierszenbaum, 2007; Ross & Pawlina, 2011).

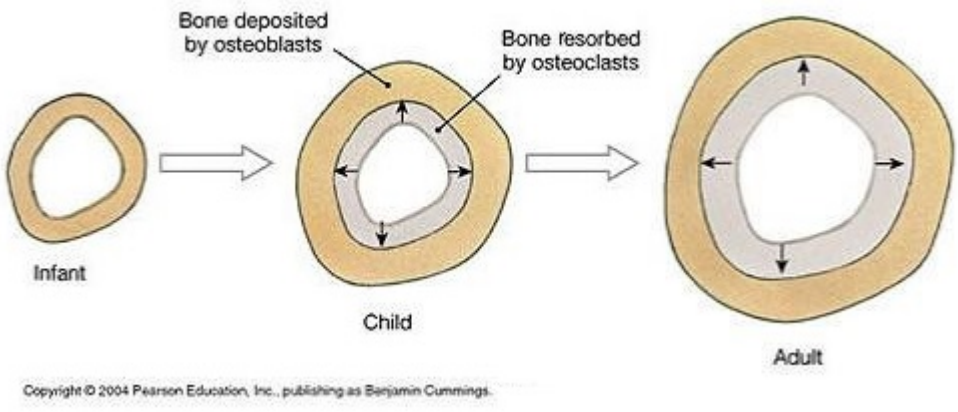

Figure 2.7 Cross section of a long bone showing appositional growth and bone resorption (Pearsons Education Inc, 2006)

2.2.3.2 Endochondral ossification

Endochondral ossification occurs when bone is formed through the replacement of a cartilage model. In this case mesenchymal stem cells will differentiate into chondroblasts and produce a cartilage model of the desired bone shape. This is done as cartilage is able to increase in bulk rapidly, which is needed in the developmental stages of pregnancy and childhood. The cartilage model will reach a maximum size at which the central chondrocytes are unable to obtain nutrients as cartilage is avascular. At this point the cells will hypertrophy and release growth factors that will attract chondroclasts and the ingrowth of blood vessels; this is known as the primary centre of ossification. Osteoprogenitor cells are transported to this primary centre where they will differentiate into osteoblasts and produce osteoid to be mineralised. In long bones, secondary ossification centres are set up in the same way at the proximal and distal ends of the cartilage model, but remain separated from the primary ossification centre by the epiphysis. The epiphysis is a region where chondroblasts remain actively proliferating and secreting cartilage on the secondary ossification centre side, and hypertrophied chondrocytes are reabsorbed and replaced with osteoprogenitors, osteoblasts and osteoid on the primary ossification side. This results in a continual lengthening of long bones during development. Once the bone has reached maximal size, the chondroblasts will cease proliferating and producing cartilage. The reabsorption of cartilage and deposition of bone matrix cycle will continue until no cartilage remains and the epiphysis region has completely been replaced with bone matrix (Kerr, 2010; Kierszenbaum, 2007; Ross & Pawlina, 2011).

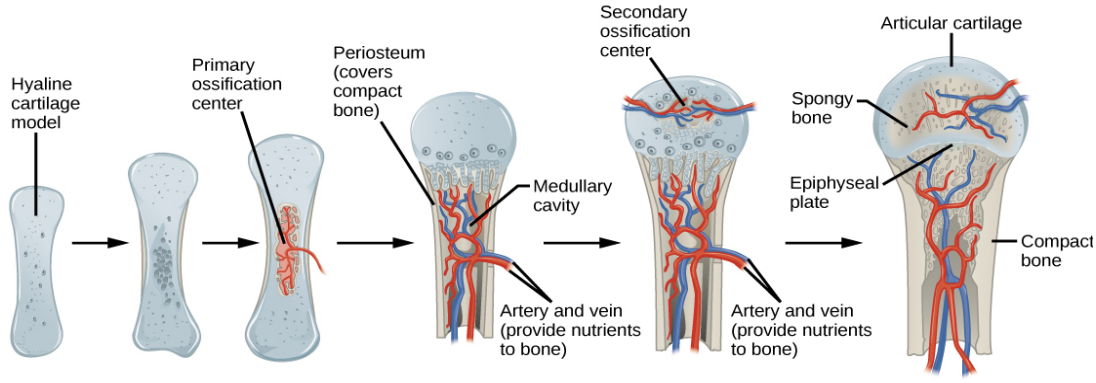

Figure 2.8 Stages of endochondral ossification (Dario-Becker, 2012)

2.2.4 Bone remodelling

Bone remodelling is an on-going process whereby old bone is resorbed and replaced with new bone without changing its overall shape. This is continually done through osteoblast-osteoclast communication to repair microcracking in the bone or old weakening bone to provide optimal bone strength (Kerr, 2010; Kierszenbaum, 2007). There are four steps in the bone remodelling process, seen here in Table 2.1:

Table 2.1 Phases of bone remodelling (Kierszenbaum, 2007)

Activation	Osteoclast precursors are recruited to the site of remodelling, and begin to differentiate into osteoclast
Resorption	Osteoclast begin to resorb the bone by phagocytosis until a lacuna has formed, and then they move away from the site
Reversal	Osteoblasts replace the osteoclast in the lacuna and begin secreting osteoid to fill the lacuna
Formation	Osteoblasts become trapped within the mineralized bone matrix and become osteocytes, finally closing off the remodelled area

Bone remodelling often occurs in response to mechanical stimuli. Mechanical stresses on the bone determine the extent of adaption the bone requires to accommodate such mechanical stresses (Bacabac & Mullender, 2005; Turner, 1998). Turner (1998) lays out rules for bone adaptions: Stimuli is a dynamic loading situation, rather than static loadings; and only short exposure periods are required to initiate the bone remodelling process. Bone remodelling is more responsive to abnormal loading conditions as the cells are less accustomed to accommodate these conditions. An example to explain this relationship is that weightlessness induces bone loss in astronauts due to the lack of loading on the bones in zero gravity (Smith & Heer, 2002).

2.2.5 Bone repair

When a bone is fractured under excessive loading it may repair itself by either endochondral ossification or intramembranous ossification:

Endochondral ossification repair occurs when there is minimal movement of the fractured bone. A cartilaginous callus is formed around the fracture for stability and to promote healing. This cartilaginous callus is gradually replaced with new bone. The callus reaches maximum size at 3 weeks, and is remodelled into bone over another 3-9 weeks depending on the extent of the breakage (Kerr, 2010; Ross & Pawlina, 2011). Intramembranous ossification repair occurs when there is a rigid surgical fixation of the fractured bone. The broken bone at the fracture site is resorbed by osteoclasts and replaced with new woven bone over the next 4-5 weeks. The woven bone will be replaced with mature bone and mineralised over the next few months to finally develop continual osteons (Kerr, 2010; Ross & Pawlina, 2011).

2.3 Implant Development and fixation

Medical implants and their designs are now able to be analytically reviewed encompassing the content in sections 2.1 and 2.2. This section will introduce the manufacturing norms of medical implants and their fixation methods. It will then

describe modifications done to the implants to make them more suitable, before outlining the design of implant samples in this study.

2.3.1 Manufacturing methods for implants

The manufacturing of medical implants has traditionally been done by methods of casting or forging following the standard specifications of the American Society for Testing and Materials (ASTM International, 2003, 2006, 2007, 2008; Hermawan *et al*., 2009). Casting is a low cost, accurate and flexible manufacturing method whereby liquid metal is poured into a mould designed to the desired shape. The mould will then be disassembled and the casting of the implant removed (Creese, 1999; Hermawan *et al*., 2009; Poli, 2001). Forging is a manufacturing method whereby the metal is deformed into the desired shape with the use of applied pressure. Forging has become a more popular method as it produces stronger forms that exhibit grain directional strength that help in preventing metal defects (Creese, 1999; Poli, 2001).

Rapid prototype development (RPD), or selective laser sintering (SLS) is fast becoming a leader in product development for its ability to construct porous surface modifications with micrometric precision. The necessity of this ability is becoming more apparent, as porous surface modification allow for better osseointegration of implants as well as the reduced possibility of stress shielding. These factors will be described more in section 2.3.3. Conventional methods are lacking the ability to precisely control internal pore sizes, interconnectivity and geometry. The technique of SLS allows the "growth" of any design by subjecting Ti64 powder to a laser for bonding, layer by layer, guided by computer aided design (CAD). Using this technique, one would easily be able to develop a detailed scaffold design as the 3D porous implant surface.

The advantages of using RPD as a development tool extend far beyond the control of surface porosity. In using RPD, one is able to produce the porous surfacing or scaffolds continuous with the solid core of the implant, as the solid core would also

be developed by the same sintering technique. This continuity would potentially prevent a defined scaffold/surface interface weak point, resulting in a stronger unit (Peltola *et al*., 2008). Another advantage of using RPD is its ability to produce patient specific implants. Using MRI images as an input, one is able to "grow" the individual implant leading to fewer problems of ill-fitting implants causing aseptic loosening (Peltola *et al*., 2008; Pfister *et al*., 2003).

2.3.2 Cemented vs Cementless debate

Over 80% of arthroplasties use what is known as a cemented implants (National Joint Registry, 2012). Cemented implants have long been used for joint replacements as they are suitable for weaker, older bones that do not repair rapidly. The cement provides strength and stability to the implant's fixation. Patients more susceptible to infection, such as the elderly, are also more suited to cemented implants as antibiotics can be delivered directly to the area via the cement (Gandhi, Tsvetkov, Davey, & Mahomed, 2009; Panagis, Saled, & Sledge, 2013). The procedure involves the application of fast curing polymethyl methacrylate medical grade cement (PMMA) to the exposed bone or within the hollowed long bone, followed by the slow and steady insertion of the prosthesis. Recovery time is good for cemented prosthesis as most patients are encouraged to weight bear on the joint in the early post-operative stages, and may be able to weight bear unaided within four weeks (Waddell, 2008). A problem tends to arise with cemented implants, in that they show excellent short term fixation but that begins to deteriorate with time (Waddell, 2008). Freeman (1976) suggests that the continued cyclical load of joints in the long term is enough to deteriorate the PMMA/bone interface connection, thus causing the fixation loss over time. The release of debris particles from the PMMA/bone connection breakdown are also likely to cause an inflammatory response and osteolysis in the region as outlined in the introduction to chapter 2, as well as contribute to abrasive particles at the joint surface, further aggravating the deterioration (Allen *et al*., 1996; Anderson, 2001; Brodbeck & Anderson, 2009; Haleem-Smith *et al*., 2012).

To reduce aseptic loosening by improving the initial fixation and stability of implants, many surgeons are tending to move away from cemented fixation implants, and are rather using cementless implants which allow for direct bone to implant osseointegration (Loew, 2013; Wilkinson, Gordon, & Stockley, 2003). Cementless implants are suitable for younger, active patients with strong, healthy bones that will be able to integrate with the implant for strength and stability. A cementless implant would be secured in place either by screw fixation, or by press fit fixation (Panagis *et al*., 2013; Waddell, 2008). Recovery time for a cementless implant is much longer than that of a cemented implant. A patient will be bed ridden for the first six weeks post operatively to avoid dislocation, and will only be able to return to normal unaided activities at 12 weeks. This lengthy recovery period is in order to allow for the regrowth of bone into the porous surface of the implant and the associated strong biological fixation to develop. Cementless implants have been seen to have a longer-term, stronger fixation that also improves with time, than that of cemented implants, and this is again why it is better suited for younger patients (Rothman & Cohn, 1990; Waddell, 2008).

2.3.3 Surface modifications to cementless implants

Studies have shown that the rate of osseointegration of cementless implants is associated with the chemical and the physical properties of the implant material (Engler *et al*., 2006; Le Guehennec *et al*., 2008, 2007; Li *et al*., 2007); these properties may be modified to improve the biological response to the implant and further encourage new bone growth (Anselme *et al*., 2000; Hermawan *et al*., 2009; Yang, Tian, Deng, & Ong, 2002).

A good example of a chemical modification to the implant is the biological coating of the metal implant with layers of calcium phosphate, or hydroxyapatite. A number of studies have shown that such a coating has an excellent osteoconducive effect and a superior long term success rate for implant fixation (Barrere *et al*., 2003; Geurs, Jeffcoat, McGlumphy, Reddy, & Jeffcoat, 2002; Morris, Ochi, Spray, & Olson, 2000). The calcium phosphate layer increases the adsorption of proteins in

the peri-implant region, and functions as a matrix for osteogenic cell adhesion and growth, accelerating the healing process (Davies, 2003).

Rough surfaces are a physical characteristic of an implant that would encourage bone anchoring and biomechanical stability by promoting the entrapment of fibrin proteins, adhesion of cells and their subsequent proliferation and differentiation into osteoblastic cells (Le Guehennec *et al*., 2008). Some of the methods used to produce rough surfaces include sintering, surface blasting and/or surface etching, plasma spraying, fine wire networks or beading (Lavenus *et al*., 2011; Le Guehennec *et al*., 2008; Perrotti *et al*., 2013; Pohler, 2000; Steinemann, 1998). Wennerberg, Albrektsson, Albrektsson, & Krol, (1995) placed Ti screw implants into a rabbit bone for 12 weeks and then observed the torque needed to remove the screws. Their results illustrated that microtopographic roughness (1-10 µm) is the best range for maximizing the interlocking of the mineralized bone and the implant surface, in turn producing a higher bone-to-implant contact ratio and resistance to torque. This rough surface range is highly beneficial in patients when the bone is of poor quality or volume and/or undergoes high levels of loading (Le Guehennec *et al*., 2007). Le Guehennec *et al*.'s work (2008) showed that biphasic calcium phosphate ceramic grit-blasted Ti (BCP-Ti) produced a suitable surface roughness with no contaminants for the adhesion and proliferation of the MC3T3-E1 cells when compared with mirror polishing Ti, alumina grit-blasted Ti and commercially available Ti implants. Perrotti *et al*.'s study (2013) compared the growth of human MSCs from bone marrow on smooth machined Ti disks, sandblasted and acid-etched Ti disks, and on high temperature sandblasted and acid-etched Ti disks. After one week, the results on the high temperature sandblasted and acid-etched Ti disk showed the down-regulation of RUNX2 and BGLAP (markers of early phase bone development), and the up-regulation of SP7 and ALPL proteins (markers of later phase bone development), and collagens, indicating that this disk was the most suitable for osseointegration as it encourage differentiation of cells quicker than other Ti disks.

Solid implants have a much higher stiffness than that of bone which can create stress shielding between the bone and the implant and result in aseptic loosening. This is the phenomenon whereby bone is resorbed during remodelling and not replenished due to its lack of loading, as the bone loadings are being transmitted through the stronger implant material (Huiskes, Weinans, & van Rietbergen, 1992). To improve the physical qualities of the implant to prevent stress shielding and encourage bone ingrowth, the introduction of porosity is important (Dabrowski *et al*., 2010). The ingrowth of bone will depend on pore sizes, shape, amount, and interconnections, however there is no consensus on what these should be (Li *et al*., 2007). In 2011, Sobral, Caridade, Sousa, Mano, & Reis seeded cornstarch/poly(ε-caprolactone) blended scaffolds with human osteosarcoma cells, and showed that the use of a pore size gradient within the scaffold created a funnelling effect on the seeded cells which doubled the cell seeding efficiency under static culture conditions. Takemoto *et al*. (2005) illustrated that osseointegration did occur *in vivo* when sintered porous bioactive Ti samples were implanted into Japanese white rabbits. After sacrificing the rabbits, the Ti samples were sectioned to observe the ingrowth of bone (Otsuki *et al*., 2006; Takemoto *et al*., 2005). Li *et al*. (2007) demonstrated similar osseointegration of Ti samples developed from 3D fibre deposition *in vivo*. The samples were implanted on L4 and L5 transverse processes of goats, and again ingrowth of bone was seen after the over 12 weeks and after euthanization. Different techniques are being used to produce this porosity including plasma spraying, shot-blasting and acid etching. However these techniques do not allow for the micro-control of pore sizes but rather produce a pore size range (Karageorgiou & Kaplan, 2005; Li *et al*., 2007).

2.3.4 Key points for current study

Ti64 implant samples in this study will be manufactured by laser sintering using the RDP process for its ability to develop specific designs. To obtain a porous surface on the implant to allow for bone ingrowth, osseointegration and possible vascularization, the implant samples used for this study will be designed and

manufactured with a 3D scaffold structure on the surface to be positioned at the bone/implant interface.

2.4 Seeding cells into Ti64 implants

Early osseointegration of Ti implants is crucial for their biological fixation and thus their long-term success. In this study it is hypothesised that if the Ti64 scaffold is impregnated with the patient's own mesenchymal stem cells (for example, from the patient's own bone marrow), this might further improve the osseointegration of the implant as mesenchyme cells have the capability to differentiate into osteoblastic cells and produce bone. The seeded cells adhering to the strands of the scaffold as well as the Ti base area will potentially be able to undergo normal bone remodelling processes with the ingrowth of host bone allowing for a secure interlocking of the implant.

Baba *et al*. (2010) has published that the pre-seeding of 3D woven fabric scaffolds with human mesenchymal stem cells prior to implantation, increased the levels of new bone formation and osseointegration almost ten-fold when compared with an unseeded scaffold implant, and four times as much when compared with scaffolds seeded on implantation.

2.4.1 Cells on Ti64

The adhesive and differentiation abilities of mesenchymal stem cells on Ti scaffolds have been investigated by previous groups, Lavenus *et al*. (2011), Maeda *et al*. (2007), and Perrotti *et al*. (2012). In 2007, Maeda *et al*. showed rat mesenchymal stem cells had similar adhesive, spreading and differentiation qualities on finely polished Ti dishes compared to that on tissue culture optimized dishes. Stiehler *et al*. (2008) used human mesenchymal stem cells to do comparison tests on Ti, tantalum (Ta) and chromium (Cr) surfaces. The Ti surface showed the highest level of proliferating cells. However, although cells on the Ti surface did differentiate, it was seen to be slower than those on Ta.

As previously mentioned the structure and porosity of Ti64 plays a role in the osseointegration of the implant. A study done by St-Pierre *et al*. (2005) tested Ti scaffolds produced by powder metallurgy with pore sizes of 336-557 µm. Their work shows that the average pore size did affect the rate of proliferation of the mouse preosteoblasts over nine days, with the smaller pore sizes encouraging proliferation. However, the rate of differentiation was unaffected, concluding that the porosity and finishing of the Ti surface did not inhibit nor encourage differentiation. Lavenus *et al*. (2011) looked at the nanometric pores of 30 nm, 150 nm and 300 nm. Their study concluded that nanopores of 30 nm could possibly promote early differentiation. One can conclude that the geometries of scaffolds affect the proliferation of the cells on Ti64, but that differentiation occurs independently, and may possibly be enhanced by nanometric roughening.

2.4.2 Seeding of a RPD implant

Although the efficiency of cells on various scaffolds and substrates have been tested and confirmed, minimal work has been done testing the efficiency of scaffolds produced using RPD techniques due to it still being a new and novel technology. However within the last decade the RPD has been developed as a state of the art technology with parts being produced showing no internal defects and high geometric accuracy (Becker & Vicatos, 2005). Low seeding efficiencies of 25-35% have been reported on rapid prototyping scaffolds (Holy, Shoichet, & Davies, 2000; Pfister *et al*., 2003; Sobral *et al*., 2011). Holy *et al*. (2000) found that 75% of rat bone marrow cells would accumulate at the bottom of the dish and not contribute to tissue development on polylactide-co-glycolide (PLGA) scaffolds. They suggested that the cell size is so miniscule when compared with the scaffold pores defined by the struts that the cells penetrate and accumulate at the bottom. It was also noted in their work, that although seeding efficiency on these scaffolds was low except near the bottom, it did not affect the overall proliferation, spreading and differentiation of the surviving cells. Pfister *et al*. (2003) showed supporting results when using an osteoblast-like cell line on polyurethane scaffolds.

Sobral *et al*. (2011) developed polyε-caprolactone scaffolds with graduated pore size to test the cell seeding efficiency. Human osteosarcoma cell lines were seeded into scaffolds and showed a 30-40% seeding efficiency on homogeneous scaffolds with a minimum pore size of 100 µm, 12 hours after seeding. In the graduated scaffold with pore sizes ranging from 100 µm to 750 µm, with the 100 µm pore size being in the centre of the scaffold, the seeding efficiency was increased to 70% 12 hours after seeding. As Sobral *et al*. (2011) points out, not only is the contact surface area important, but pore structure and size play an important role in cell migration and adhesion.

2.4.3 Ti64 heat treatment effects on cells

Heat treatment, or thermal oxidisation of Ti64 have shown to have vast mechanical improvements on the material, and it has shown to have no significant effect on the adhesion of mesenchymal stem cells (García-Alonso *et al*., 2003). García-Alonso *et al*. (2003) thermally oxidised Ti64 at 500 °C and 700 °C for one hour in order to test its effects on human osteoblastic cell attachment. Results showed that the thermal oxidisation process did not inhibit cell attachment, conversely, for the initial two hours of attachment, cells had a better seed efficiency on the heat treated Ti64, notable the 700 °C treatment, compared with the untreated Ti64. Subsequent work done by Saldaña, Vilaboa, Vallés, González-Cabrero and Munuera (2005) showed that the 700 °C heat treatment increased surface roughness and encouraged cell attachment. Their study went further to look at cell proliferation and differentiation on the heat treated Ti64. Ti64 heat treated at 700 °C showed slower proliferation initial, but showed comparable values at day seven to 500 °C treated Ti64 and the untreated Ti64. After one week, the differentiation was highest on the 500 °C treated Ti64, followed by the 700 °C treated Ti64 and then the untreated Ti64 (Saldaña *et al*., 2005). These results again agreed with García-Alonso *et al*.'s (2003) original conclusion that the thermal oxidation of Ti64 had no hindering effect on the adhesion of mesenchymal stem cells.

3 Aims and objectives

In this study, it is hypothesised that the seeding of three dimensional (3D) scaffold structures with cells that are able to differentiate and produce bone will improve the potential for osseointegration of the implants.

The aim of this study is thus to investigate the effect that the thermal oxidization, or heat treatment process on the laser sintered 3D Ti64 scaffolds will have on the potential for adhesion, proliferation and differentiation of the seeded mesenchymal stem cells *in vitro*.

This will be done by:

- Subjecting the Ti64 scaffolds to a heat treatment of 600 °C for 20 hours based on Mudd *et al*.'s (2003) findings
- Assessing the cell adhesion, growth and differentiation on the untreated and heat treated Ti64 scaffolds
- Comparing the results of untreated and heat treated Ti64 tests to assess the effects heat treatment has on the cells capabilities.

4 Methods and Materials

4.1 Ti64 Scaffolds

Ti64 disks were designed with a scaffold surface at the University of Cape Town (UCT) using SolidWorks software. The scaffold structure was made up of inverted tetrahedral shapes to provide a three dimensional structure and to increase the surface area. The design was manufactured at the Centre for Rapid Prototyping and Manufacturing (CRPM) of the Central University of Technology (CUT) in Bloemfontein using an EOSINT M280 machine. The scaffold design was selectively laser sintered from Ti64 powder using a 200 Watt solid state fibre laser in an optimal protective argon atmosphere supplied at 100 litres per minute under 400 kPa. After manufacturing, the scaffolds were etched to prepare the surface for cell culture work. Scaffolds were submerged in Krolls reagent (6% nitric acid, 2% hydrofluoric acid, 92% distilled water) for 30 seconds, followed by a thorough rinsing under tap water to stop the corrosion reaction. Scaffolds were sonicated for five minutes in a water bath to loosen any trapped residue, and were finally rinsed well with distilled water.

4.1.1 Cell culture preparation

Prior to any cell culture experiments, the scaffolds were place in Trypsin/EDTA (final concentrations of 0.05% / 0.02% respectively) (Biowest) for approximately 10 to 20 minutes to dissociate any protein bonds. Scaffolds were washed with EXTRAN MA 03 phosphate-free detergent (Merck chemicals) and rinsed well with distilled water. Each scaffold was finally wrapped individually in foil and autoclaved at 121 °C and 103 kPa for 15 to 20 minutes for sterilization.

4.1.2 Thermal Oxidisation

Thermal oxidisation of scaffolds was done at the Department of Materials Engineering at UCT. The heat treatment was done in air at 600 °C for 20 hours in a Naber D2804 furnace on a clean ceramic brick. Scaffolds were allowed to cool to room temperature before removing from furnace. Samples were etched with Krolls

reagent as described earlier, cleaned and prepared again for cell culture as outlined above.

4.2 Tissue Culture

All cell work was done in a Bio-Flow Biological Safety Cabinet class 2. Cells were incubated in a Forma Scientific water-jacketed incubator at 37 °C in 5% CO_2. All work equipment and surfaces were sterilised using 70% ethanol, and sterile surgical gloves were worn at all times. Microscopy was done on an Olympus CKX41 phase contrast microscope and a Zeiss Axiovert 200M fluorescence microscope.

4.2.1 Source of rat mesenchymal stem cells

Rat mesenchymal stem cells (rMSCs) were obtained from the Cardiovascular Research Unit at UCT. The cells were isolated from bone marrow, and MSC lineage was confirmed by testing for osteogenic differentiation using Alizarin red stain, and adipogenic differentiation using Nile red stain. rMSCs were received at passage number 2 and stored in frozen cryovials in liquid nitrogen for further use.

4.2.2 Source of human mesenchymal stem cells

Human mesenchymal stem cells (hMSCs) were obtained from the Institute of Cellular and Molecular Medicine at the University of Pretoria where they were isolated from adipose tissue. The cells' mesenchymal lineage was characterised by (i) their ability to adhere to plastic, (ii) their expression of the following markers: CD73, CD90, and CD105 (these markers were >95% positive); while lacking expression of CD34 and CD45 (<5%), as measured by flow cytometry, and (iii) their ability to differentiate into adipose, bone and cartilage lineages. The isolated hMSCs were received in a frozen cryovial on dry ice in two batches; the first at passage number 10, the second at passage number 3 at passage, and stored in liquid nitrogen for further use.

4.2.3 Source of human fibroblast cells

Human fibroblast cells (hFibs) were obtained from the REDOX research group at UCT from donated neonatal foreskins obtained from elective circumcision procedures done at the Kingsbury Hospital. Small fragments of the skin were cultured under coverslips until an outgrowth of hFibs was obtained. Isolated cells were received at passage number 3 and stored in liquid nitrogen for further use.

4.2.4 Culturing of MSCs and hFibs

Cells were thawed in order to culture and bulk up the number of cells for experiments. The thawing procedure of cells is outlined in Appendix B.1: Thawing of MSCs. An optimal growth density, according to literature (ATCC, 2011, 2012; Meinel *et al.*, 2004; Thermo Fisher Scientific Inc. & Kamath, 2009) of 5,000 cells/cm^2 was used for MSCs. The thawed cells were maintained in a standard culture medium[1], following the protocol outlined in Appendix B.2: Maintenance of MSCs in Standard culture medium. Once the cells reached 80-90% confluency, they were passaged following the passaging method described in Appendix B.3: Passaging of MSCs using Trypsin/EDTA (final concentrations of 0.05% / 0.02% respectively) (Biowest), and resuspended at a density of 5,000 cells/cm^2. Cells were counted following section 4.2.6 and viewed using phase contrast microscopy to observe growth over 21 days.

4.2.5 Differentiation of MSCs

After passaging, MSCs were resuspended in the initial standard culture medium[2] at a recommended differentiation density of 10,000 cells/cm^2 (Lavenus *et al.*, 2011; Le Guehennec *et al.*, 2008; Maeda *et al.*, 2007; Marion & Mao, 2006; Sotiropoulou,

[1] Standard culture medium: for rat cells: Dulbecco's modified Eagle medium (DMEM), 10% foetal bovine serum (FBS) and antibiotics; for human cells: alpha Minimum essentials medium (αMEM), 10% FBS and antibiotics (see recipes in Appendix A. **Tissue culture medium Recipes**)

[2] Standard culture medium: for rat cells: Dulbecco's modified Eagle medium (DMEM), 10% foetal bovine serum (FBS) and antibiotics; for human cells: alpha Minimum essentials medium (αMEM), 10% FBS and antibiotics (see recipes in Appendix A. **Tissue culture medium Recipes**)

Perez, Salagianni, Baxevanis, & Papamichail, 2006). After allowing cells to settle for 48 hours, standard culture medium[1] was suctioned off cells and replenished with osteogenic medium[1]. This protocol is outlined in more detail In Appendix B.4: Osteogenic differentiation of MSCs. The differentiating cells were maintained for up to 26 days. Cells were counted following section 4.2.6 and viewed using phase contrast microscopy throughout the differentiation process.

4.2.6 Counting of MSCs

After passaging, MSCs were resuspended in standard culture medium[1]. The cell suspension was pipetted into a haemocytometer for counting. The average number of counted cells was then multiplied by the volume of medium used in suspension to obtain the total number of cells. The total number of cells were then used to plot a growth curve of the cells in order to determine their rate of growth, or doubling time, using the method described in Kruse & Patterson (1973).

4.2.7 Freezing of MSCs

Once a sufficient number of cells were obtained, they were frozen down in batches following the protocol described in Appendix B.5: Freezing of MSCs, for storage in liquid nitrogen until needed for experimental work on Ti64 scaffolds.

4.3 Tissue culture work on Ti64 scaffolds

All methods done on Ti64 scaffolds are replicable for rMSCs and hMSCs experiments. However, rMSC experiments were duplicated, with a third scaffold being stained for microscopy observations when required, whereas hMSC experiments were done using one scaffold, due to the constraint of cell numbers. The scaffolds were stained for microscopy observation prior to passaging when required.

[1] Osteogenic medium: DMEM, 10% FBS and antibiotics with osteogenic supplements, Ascorbic-2-phosphate, β-glycerophosphate and dexamethasone (see recipe in Appendix A. **Tissue culture medium Recipes**)

4.3.1 Seeding and culturing of MSCs on scaffolds

After passaging, MSCs were resuspended in standard culture medium[1] and pipetted on top of each scaffold to form a meniscus. The scaffold and meniscus were incubated and left undisturbed to allow for the settling of cells onto the Ti64 for a specified amount of time tested and determined in section 5.2. The scaffolds were then flooded with standard culture medium[1] until the scaffolds were fully submerged as described in the protocol in Appendix C.1: Seeding MSCs on Ti64 scaffolds. The same optimal growth density of 5000 cells/cm^2 was used for MSCs on the scaffolds as was used on the tissue culture dishes. The scaffolds were cultured following the protocol outlined in Appendix C.2: Maintenance on Ti64 of MSCs in Standard culture medium for up to 21 days to observe the growth of the cells on the Ti64 substrate.

4.3.2 Osteogenic differentiation of MSCs on scaffolds

For differentiation experiments, the standard culture medium[2] was changed to osteogenic medium[3] two days after the seeding of cells onto the scaffolds. This protocol is outlined in Appendix C.3: Osteogenic Differentiation maintenance on Ti64. The scaffolds were maintained and their proliferation and differentiation was observed at various time-points over a 26 day period through the counting of cells and though fluorescence microscopy imaging, similar to what was done for the cells on the tissue culture dishes.

---

[1] Standard culture medium: for rat cells: Dulbecco's modified Eagle medium (DMEM), 10% foetal bovine serum (FBS) and antibiotics; for human cells: alpha Minimum essentials medium (αMEM), 10% FBS and antibiotics (see recipes in Appendix A. **Tissue culture medium Recipes**)

[2] Standard culture medium: for rat cells: Dulbecco's modified Eagle medium (DMEM), 10% foetal bovine serum (FBS) and antibiotics; for human cells: alpha Minimum essentials medium (αMEM), 10% FBS and antibiotics (see recipes in Appendix A. **Tissue culture medium Recipes**)

[3] Osteogenic medium: DMEM, 10% FBS and antibiotics with osteogenic supplements, Ascorbic-2-phosphate, β-glycerophosphate and dexamethasone (see recipe in Appendix A. **Tissue culture medium Recipes**)

4.3.3 Passaging of cells from scaffolds

In order to observe the proliferation of cells on the scaffolds, the cells were harvested from the scaffolds and counted in a haemocytometer as described in section 4.2.6. At particular time points over a 26 day period, cells were passaged from scaffolds following the protocol outlined in Appendix C.4: Passaging MSCs on Ti64 scaffolds. Scaffolds were washed repeatedly, in order to obtain the maximum number of cells for counting.

4.3.4 Microscopy observation of cells in scaffolds

As the Ti64 scaffolds are solid and opaque, imaging of the cells could not be done with a phase contrast microscope. Fluorescence microscopy was done using fluorescent stains to highlight the point of interest. The fixation of cells was decided against, as the chemicals in the fixation process may affect the scaffolds for repeated use, thus LIVE staining was used on cells within the scaffolds.

Alizarin Red LIVE stain medium[3], was used to stain the calcium deposits produced by the differentiated osteoblasts. Hoechst LIVE stain medium[4], was used to stain the nuclei of cells within the scaffolds. The protocol for staining the cells is described in Appendix C.5: Staining osteogenic differentiation on Ti64 scaffolds.

[3] Alizarin Red LIVE stain medium: Alizarin Red S powder stain dissolved in standard culture medium (see recipes in Appendix A. **Tissue culture medium Recipes**)

[4] Hoechst LIVE stain medium: Hoechst 33342 fluorescent stain dissolved in phosphate buffer solution (PBS) (see recipes in Appendix A. **Tissue culture medium Recipes**)

5 Results

5.1 Design and heat treatment of Ti64 scaffolds

The first step was to manufacture a suitable Ti64 scaffold to use for cell experimentation. Solid Ti64 disks were initially manufactured to a diameter size of 22 mm using the process of laser sintering. In the same process, an inverted tetrahedral scaffolding structure was developed on one side of the disk to provide a more three dimensional surface thus increasing the surface area for cell attachment, and allowing for improved ingrowth and interlocking of bone in clinical applications. The scaffolding structure was made up of struts with a 0.7 mm thickness and thus forming pores of approximately 0.5 mm across corners. This scaffold structure design is shown in Figure 5.1 A and B. The addition of this scaffolding structure on the 22 mm diameter disk increased the surface area from 3.80 cm^2 to 11.17 cm^2. After the first set of tests, a second batch of Ti64 disks were manufactured, but with a diameter of 18 mm in order to fit into smaller tissue culture dishes. The scaffolding structure increased the surface area from 2.54 cm^2 to 8.29 cm^2 for these 18 mm diameter disks. The decrease in disk diameter did not affect the results obtained in cell tests, and it was purely changed to enhance ease of use. Both disk sizes were continued to be used in experiments and the difference in surface areas were taken into account when seeding cells.

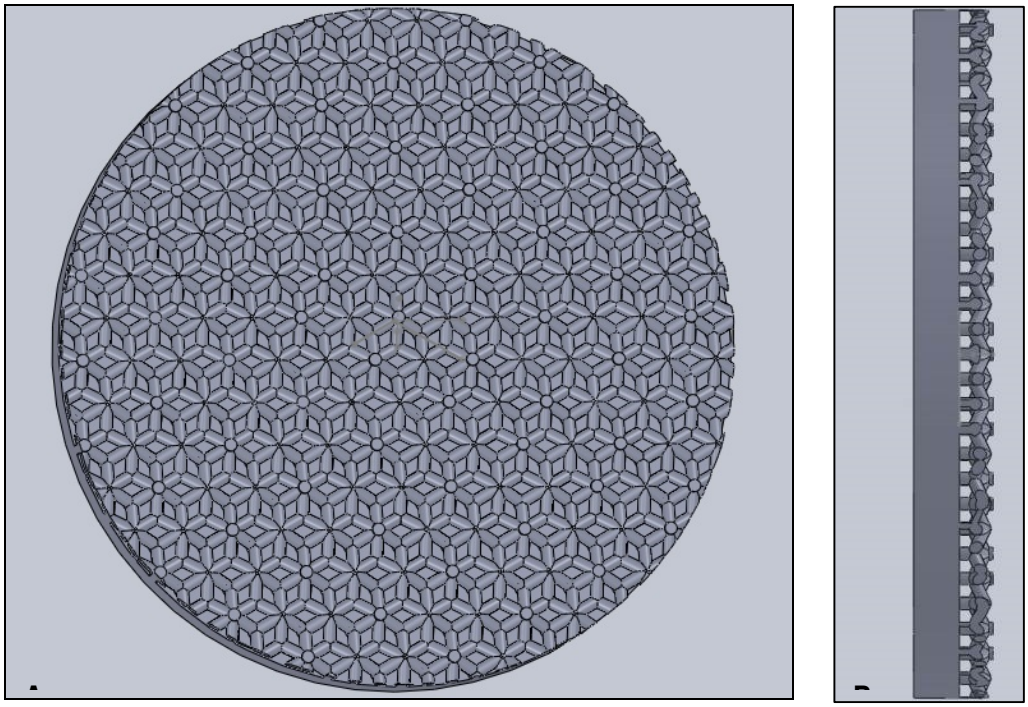

Figure 5.1 Structural design of Ti64 scaffolds: (A) Top view and (B) side view

In order to prepare the Ti64 for subsequent cell work experiments, the scaffolds had to undergo the heat treatment process to create the appropriate substrate. All scaffolds that were heat treated were placed in the Naber D2804 furnace and brought up to a temperature of 600 °C and maintained there for 20 hours. After the heating time period, the scaffolds were allowed to cool to room temperature prior to removing from the furnace. After the heat treatment process, a pleochroic rutile surface was seen on the scaffold disks, whereby the substrate appears to have had a colourmetric change, as seen on the left of Figure 5.2. This is a form of naturally occurring TiO_2, and due to its presence one is able to confirm the success of thermal oxidisation of the substrate.

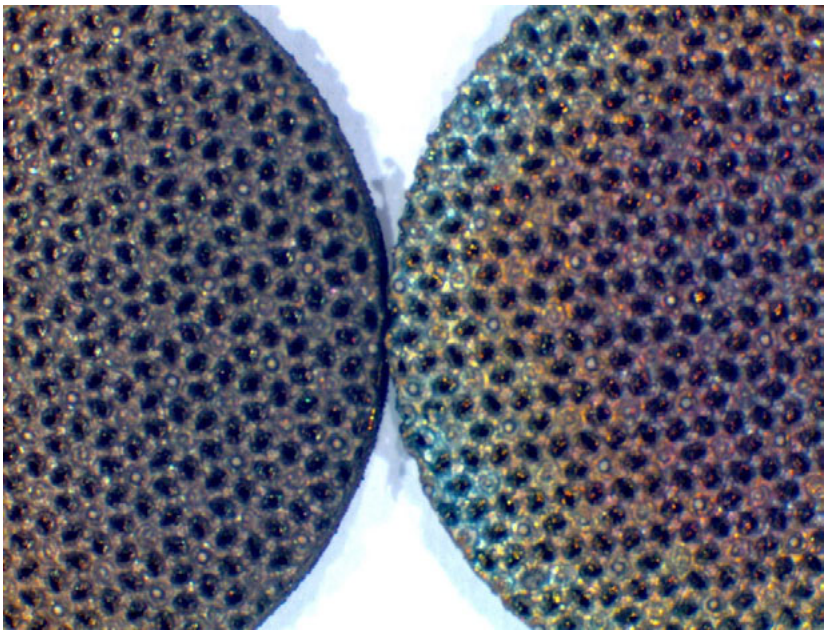

Figure 5.2 Image showing the naked eye appearance of the untreated Ti64 substrate (left) and the heat treated (B) Ti64 substrate (right)

In order to visualise any differences in the topography of the untreated and heat treated Ti64 substrates, stereoscopic images were taken. These images are presented in Figure 5.3, and show both the surfaces of the base of the scaffolds, as well as that of the scaffold struts. In the image of the base of heat treated scaffold, striations on the substrate were seen; these were seen on the base of the untreated scaffolds as well, but images clearly showing this were difficult to obtain. The striations seen on the scaffold bases were likely from the laser sintering manufacturing process, and provide an additional roughening to the substrate. The struts of the scaffolds were easier to view, and one can see that the roughened topography obtained through the sintering development process in the untreated images was unchanged in the heat treatment images. This suggests that the heat treatment process does not change the surface topography, but merely the chemical microstructure when oxidised.

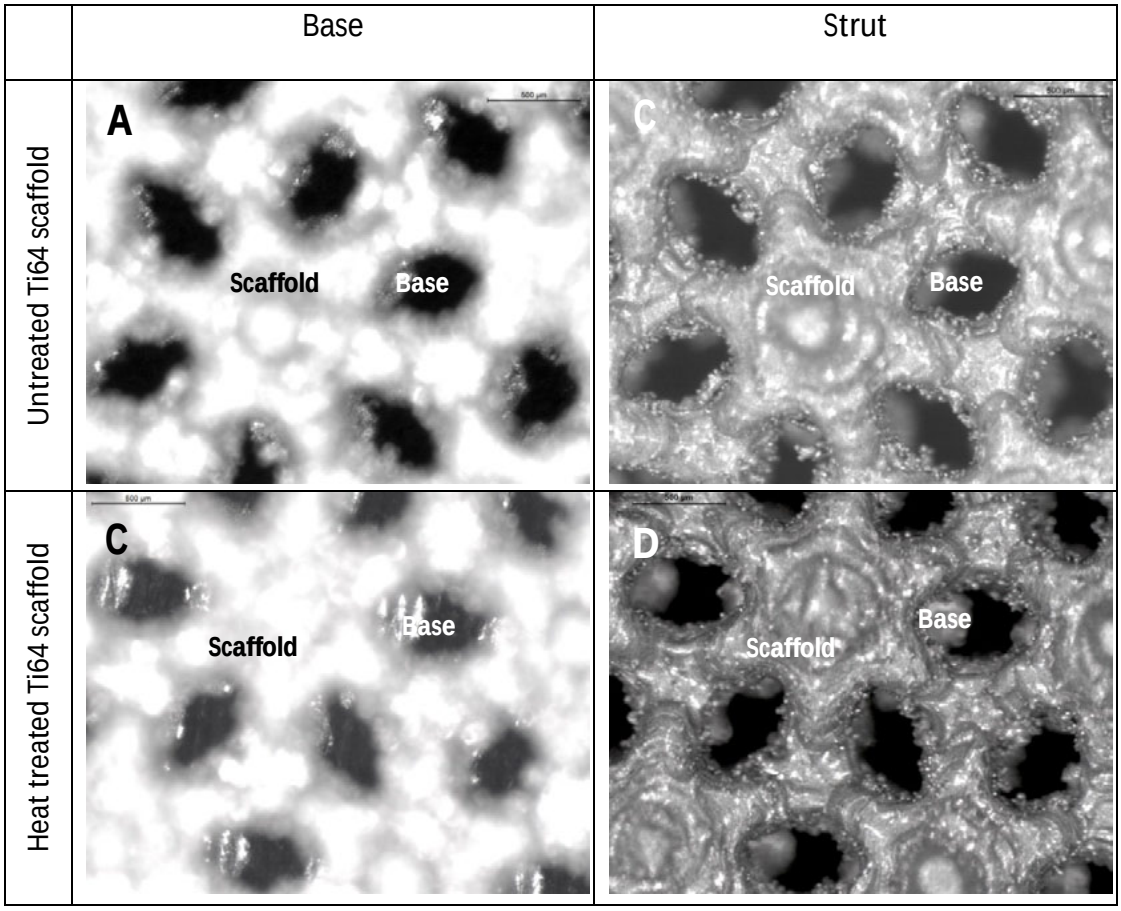

Figure 5.3 Stereoscopic images of Ti64 substrate characteristics. A and B show the surface topography of the untreated Ti64 and C and D show that of the heat treated Ti64. A and C show the base surface of the respective Ti64 substrates, where the struts are seen as bright and unfocused. B and D show the struts surface of the respective Ti64 substrates, where the base is seen unfocused.

5.2 Pilot study to test the seeding efficiency of cells on Ti64 scaffolds

The first challenge in this study was to determine the best way in which to seed the cells into the scaffolds and to determine the seeding efficiency. In the first pilot run, $20x10^4$ human fibroblasts (hFibs) were seeded in 0.5 ml standard culture medium (DMEM with 10% foetal bovine serum; quantities as per Appendix A. Tissue culture medium Recipes) onto sample disks of Ti64 scaffolds and incubated for one to three hours at 37 °C prior to flooding the scaffold with the same culture medium. Twenty four hours later the cells were harvested and counted using a haemocytometer; the

results are listed below in Table 5.1. Two additional variables were also tested as denoted in the table. The (*) denotes that the scaffold was wet with culture medium prior to seeding of cells, and the (#) denotes that the cells were seeded into the scaffold using a syringe needle.

Table 5.1 Seeding techniques tested for optimisation on sample Ti64 scaffolds; (*) scaffolds were pre-wet prior to pipetting cells on; (#) cells were seeded onto scaffolds using a syringe and needle (n=2 for each test)

Cell type	Scaffold type	Hours from seeding to flooding of scaffold	Seeding no. of cells ($x10^4$)	Remaining no. of cells after 24hours ($x10^4$)	% Seeding efficiency
hFibs	Samples of untreated scaffolds	1	20	10.94	54.70
		2 *	20	10.06	50.30
		2	20	10.25	51.25
		2 #	20	5.19	25.95
		3	20	5.35	26.75

As can be seen in Table 5.1, scaffolds that were flooded with culture medium 1-2 hours after the initial seeding appeared to have the highest survival rate, or seeding efficiency, of between 50-55% 24 hours later. The technique of wetting the scaffolds prior to seeding, as denoted by (*) did not show an increase in the seeding number. Neither did the use of seeding the cells using a syringe needle (#), as this showed a much lower seeding efficiency. The low survival of cells in scaffolds with 3 hours of incubation before flooding is likely due the evaporation of the seeding droplet and the consequential drying out of cells.

Having established a baseline seeding efficiency with the hFibs on the sample scaffolds, the experiment was repeated on the scaffolds designed and manufactured for experimentation, as described in section 5.1. These scaffolds differed from the samples in size and in that the scaffolding structure was placed within the Ti64 disk, rather than on top, essentially enclosed by “walls” that would retain the cells. The experimental scaffolds were seeded with $20x10^4$ hFib cells and analysed 24 hours later as previously done to assess any difference in seeding

efficiency. As shown in Table 5.2, the result revealed a 41% seeding efficiency. This lower seeding efficiency shows that the sample scaffolds were able to retain more cells by the enclosing of the scaffold structure. Nevertheless, since it would not be possible for the "walled" scaffolds to be used in future clinical applications, it was considered appropriate to proceed with the open-edged scaffold design.

Using the method of seeding established for the hFibs, an experiment was run to determine the seeding efficiency of rat mesenchymal stem cells (rMSCs) seeded onto the untreated and heat treated experimental Ti64 scaffolds. The results in Table 5.2 show that for rMSCs (passage number 6) on untreated Ti64 scaffolds the seeding efficiency was 40%, and for that on the heat treated Ti64 scaffolds was approximately 36%. These results show that seeding efficiency of rat MSCs was slightly better on the untreated Ti64 than on the heat treated, but not considerably so. The passage number of cells indicates the age of cells in culture, where passage zero would be primary cells harvested from tissue. All rMSCs tests reported on in this study used passage number 6 rat MSCs.

Table 5.2 Seeding efficiencies for hFibs (n=4) and rMSCs on the untreated (n=3) and heat treated (n=5) experimental Ti64 scaffolds

Cell type	Scaffold type	Seeding no. of cells ($x10^4$)	Remaining no. of cells after 24hours ($x10^4$)	% Seeding efficiency	Average % Seeding Efficiency
hFibs	untreated	20	6.1875	30.94	40.86
		20	8.125	40.63	
		20	9.94	49.70	
		20	8.438	42.19	
rMSCs	untreated	1.34	0.4875	36.38	40.47
		0.5	0.2292	45.84	
		1.32	0.51745	39.20	
rMSCs	heat treated	1.39	0.5078	36.53	35.83
		1.809	0.6768	37.41	
		1.39	0.473	34.03	
		1.34	0.4737	35.35	
		2.39	0.959	40.13	

5.3 Growth and proliferation of rat MSCs on Ti64 scaffolds

The next step was to determine whether the rMSCs were able to grow and proliferate on the untreated and the heat treated Ti64 scaffolds. Taking previous recommendations (ATCC, 2011, 2012; Meinel *et al*., 2004; Thermo Fisher Scientific Inc. & Kamath, 2009) and seeding efficiency into account, the scaffolds were populated with rMSCs to a density of 5000 cells/cm^2. For growth studies on the untreated Ti64 scaffolds, sixteen scaffolds were seeded with rMSCs and duplicate samples were harvested at eight different time points over three weeks. This entire experiment was then repeated, again with sixteen scaffolds, with duplicate samples at eight different time points over three weeks. The results from the two separate runs were averaged and presented in Figure 5.4. For studies on the heat treated scaffolds, twelve scaffolds were seeded with rMSCs and duplicate scaffolds were harvested at six different time points over three weeks. This entire experiment was then repeated, with one scaffold harvested per time point. The results from the two separate runs were averaged and presented in Figure 5.4. As controls, cell growth was measured on standard plastic tissue culture dishes seeded at 5000 cells/cm^2. A total of eight 35 mm dishes were seeded, with one dish being harvested for each of eight time points.

The results of the rMSCs growth on the untreated and heat treated Ti64 scaffolds, and in culture dishes can be seen in Figure 5.4. The doubling time was calculated for each graph in Figure 5.4; it was found that the doubling times during the cells growth phase were approximately two and three days for the tissue culture dishes and the Ti64 scaffolds (both untreated and heat treated) respectively. This indicates that cells proliferate slightly slower on the scaffolds than on the dishes, and approximately at the same rate on both untreated and heat treated scaffolds.

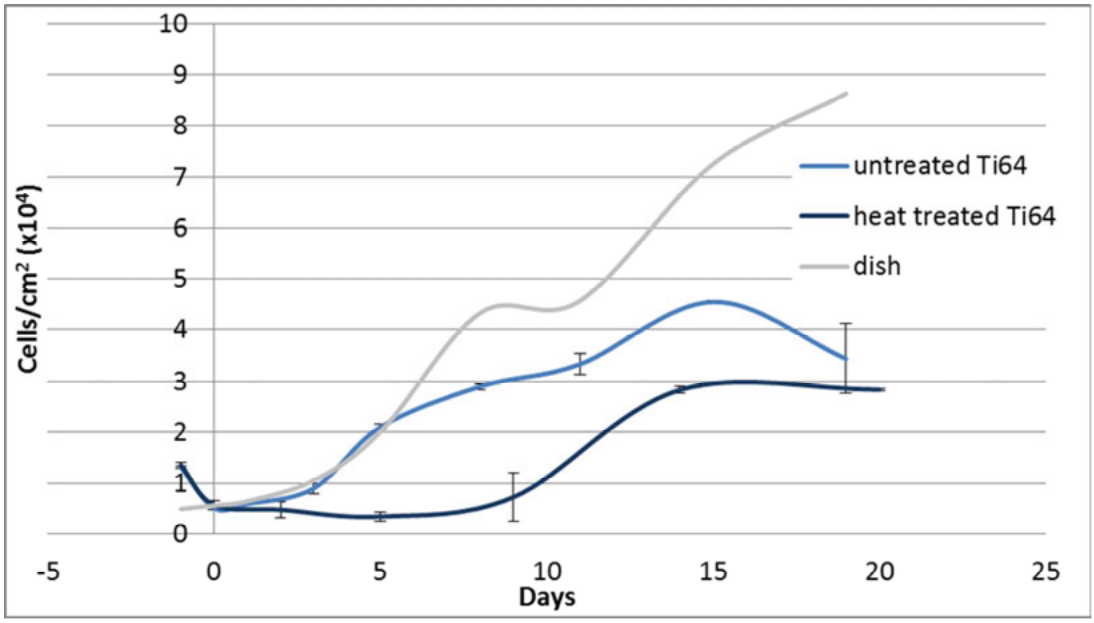

Figure 5.4 Proliferation of rMSCs on untreated Ti64 (n=4), heat treated Ti64 (n=3) and tissue culture dishes (n=1). No statistical analysis was done for growth on tissue culture dishes

The cells on both the untreated and heat treated Ti64 either reached a maximum or a plateau by day 16, yet continued to proliferate on the cell culture dishes. Theoretically the cells should continue to grow as the scaffold area for growth is greater than the area of the cell culture dish (as calculated in section 5.1). It was hypothesized that more cells were settling and adhering to the base of the scaffold, resulting in confluency of cells occurring earlier than predicted. To understand if this was indeed the circumstance, the location of the cells within the scaffolds were observed. The cell nuclei were stained with Hoechst LIVE stain (protocol and concentration as per section 4.3.4) and visualised under fluorescence microscopy one day after seeding. The results seen in Figure 5.5 show scaffolds, both untreated and heat treated, to have a greater number of cells settled on the base, with a variable number of cells on the struts. These imaging results thus support the hypothesis of the cell location causing early confluency. This would help explain the plateau in cell growth and the drop in cell count as confluent cells began to die and slough off.

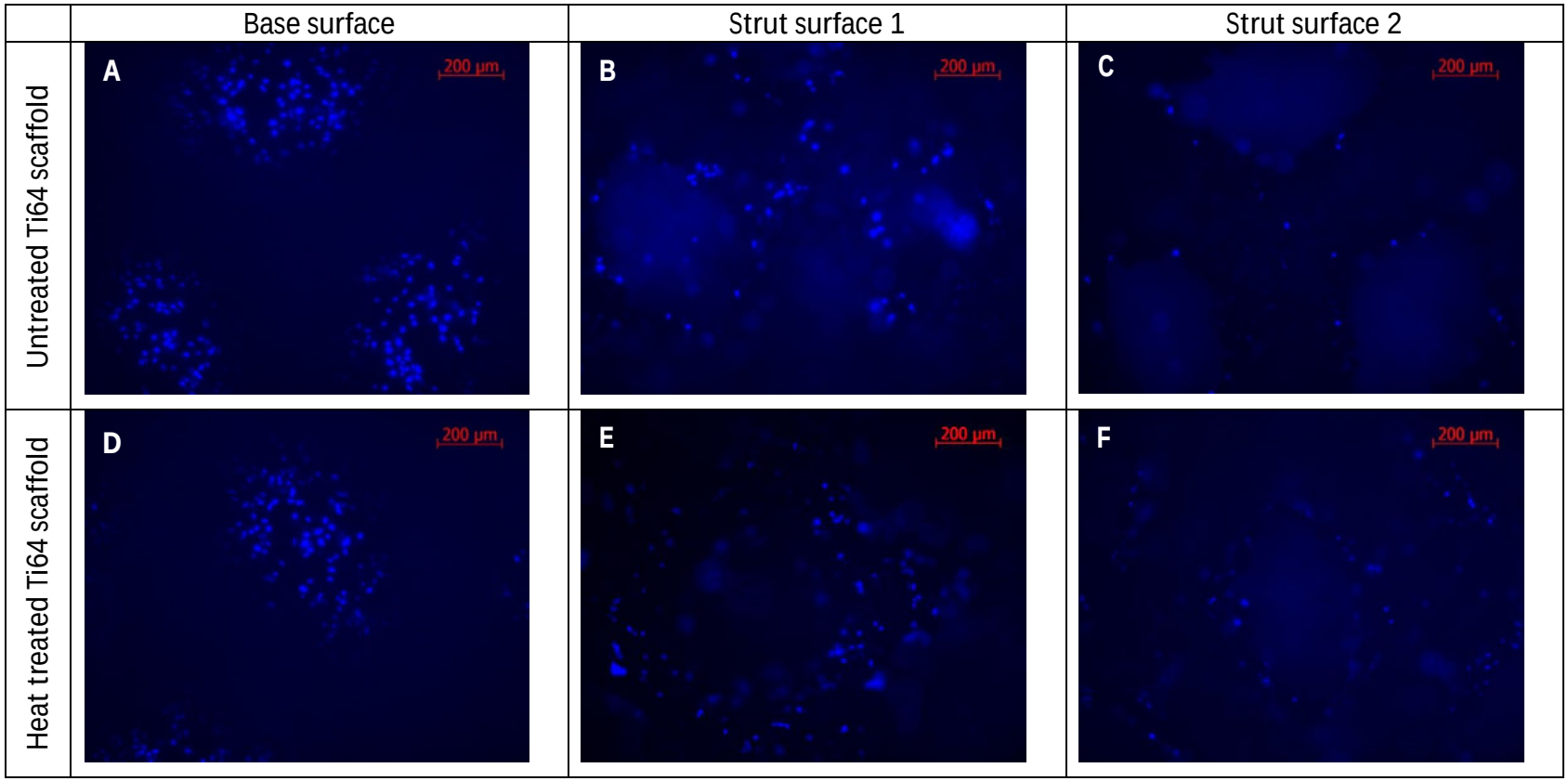

Figure 5.5 Fluorescence microscopy images of rat MSCs locations on the Ti64 scaffolds. Cell nuclei have been stained blue with Hoechst LIVE stain. A, B and C represent the rMSCs on the untreated Ti64 scaffolds. D, E and F represent the rMSCs on the heat treated Ti64 scaffolds. A and D show cells adhered to the base of the scaffolds, where the dark areas of image are out of focus struts. B, C, E and F show cells adhered to the struts where B and E show higher confluency than C and F.

Particularly noted was that the number of cells on the struts was highly variable. For example, Figure 5.5 B and D showed a greater number of cells adhering to the scaffold struts, whereas C and E showed almost no cells on the struts. This variability was seen on both the untreated and heat treated scaffolds throughout all experiments done. Further studies would need to be done to determine a seeding technique which would give consistent results for the ratio of cells on the struts compared with the base.

In summary, the rMSCs showed growth on both the untreated and the heat treated Ti64 scaffolds. The growth on the Ti64 scaffolds was slightly slower, showing a three day doubling time on both the untreated and heat treated Ti64, compared with the two day doubling time of the cells on the dishes. Finally, the cells were able to adhere to both the base and the struts of both scaffold substrates, however majority of cells settled onto the base of the scaffold, leading to earlier confluency.

5.4 Differentiation of rat MSCs into osteoblasts on Ti64 scaffolds

Having established that the rMSCs were able to adhere and proliferate on the untreated and heat treated Ti64 scaffolds, the next step was to determine whether the rMSCs were able to differentiate into active osteoblasts and produce bone matrix on the untreated and heat treated Ti64 scaffolds. Taking the seeding efficiency into account and based on previous reports (Lavenus *et al*., 2011; Le Guehennec *et al*., 2008; Maeda *et al*., 2007; Marion & Mao, 2006; Sotiropoulou *et al*., 2006), the scaffolds were populated with rMSCs to a density of 10,000 cells/cm^2 in standard culture medium. Cells were allowed to settle and adhere to scaffolds for 48 hours; the medium was then suctioned off and replaced with differentiation medium (DMEM with 10% foetal bovine serum supplemented with bone differentiation factors as described in section 4.3.2).

To establish the extent of differentiation of the rMSCs, an endpoint experiment was first carried out where rMSCs were cultured in osteoblast differentiation medium for 26 days. At the end of the culture period the scaffolds were stained with Alizarin

LIVE to visualise calcium deposits, and Hoechst to visualise cell nuclei (protocol and concentration in section 4.3.4). A semi-quantitative analysis of osteoblast activity was done on 6 different microscopy images of the base of the scaffolds at day 26. Each image was scored on the amount of calcium nodules seen and the strength of the staining, where (+++) is the highest and (+) is the lowest; and the number of cells present were counted. The results for this analysis are shown in Table 5.3, and an example of the images analysed are seen at day 26 in Figure 5.6.

Table 5.3 Semi-quantitative analysis of rat osteoblast activity at day 28 on Ti64 scaffolds. (+) denotes low, (++) denotes medium and (+++) denotes high

Scaffold	Site no.	No. of nodules	Average	Strength of staining	Average	No. of cells	Average no. of cells
Untreated Ti64	1	+++	+++	+++	+++	17	32.3 ± 11.4
	2	+++		+++		43	
	3	+++		+++		48	
	4	+++		+++		25	
	5	+++		++		30	
	6	++		+++		31	
Heat treated Ti64	1	++	++	+++	+++	38	37.3 ± 15.2
	2	++		+++		65	
	3	++		+++		24	
	4	++		+++		23	
	5	+++		++		35	
	6	++		+++		39	

The results in Table 5.3 show that a slightly greater number of calcium nodules were seen on the untreated Ti64 than on the heat treated, even though the strength of staining was comparable on the different substrates. The results also show that there was a slightly greater number of cells on the heat treated Ti64 than on the untreated, but not notably so. Considering that there were slightly more nodules seen on the untreated scaffolds, with slightly fewer cells, it may be possible to suggest that rat MSCs might be more inclined to differentiate into active osteoblasts on the untreated Ti64 scaffolds. This would however, need further testing to confirm.

Following the endpoint experiments, 21 untreated Ti64 scaffolds were seeded with rMSCs for a time-course study involving culture in differentiation medium for 21 days. Cells on scaffolds were stained with Alizarin LIVE and Hoechst stains and harvested in triplicate at seven different time points over the three weeks. This entire experiment was then repeated, again with 21 scaffolds, with triplicate samples at seven time points over three weeks. Fluorescent microscopy results seen in Figure 5.6 show the progression of differentiation on the scaffolds. For a time-course study carried out with the rMSCs on the heat treated Ti64 scaffolds, the cells were again cultured in differentiation medium for 21 days on 21 scaffolds. Cells on the scaffolds were stained as outlined above and harvested in triplicate at seven different time points over the three weeks. The entire experiment was then repeated, as with the untreated Ti64, but with only one scaffold for each of five time points. Fluorescent microscopy results seen in Figure 5.6 show the progression of differentiation on the scaffolds. As controls, cell differentiation was measured on standard tissue culture dishes seeded at the recommended (Lavenus *et al*., 2011; Le Guehennec *et al*., 2008; Maeda *et al*., 2007; Marion & Mao, 2006; Sotiropoulou *et al*., 2006) 10,000 cells/cm^2. A total of seven dishes were seeded, with one dish being stained at each of seven time points. Cells were stained with Alizarin LIVE to view the progression of differentiation using phase contrast microscopy, and results can be seen in Figure 5.6.

	Untreated Ti64 scaffold		Heat treated Ti64 scaffold		
Day	Base surface	Strut surface	Base surface	Strut surface	Tissue Culture dish
0	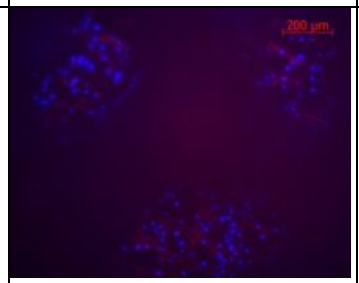	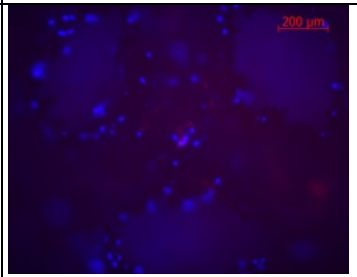	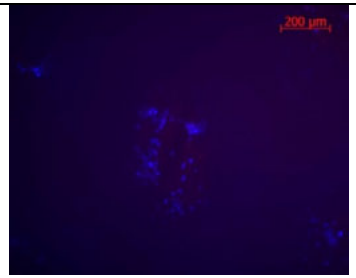	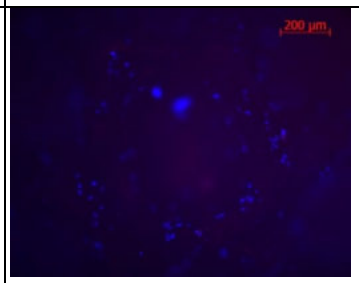	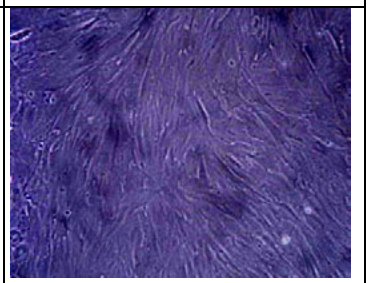
3	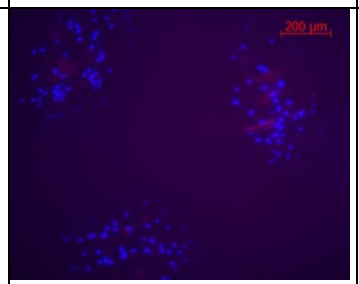	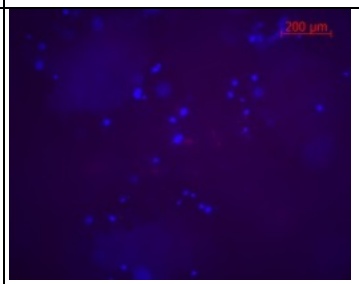	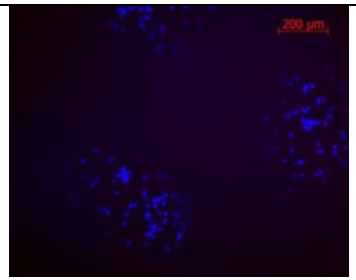	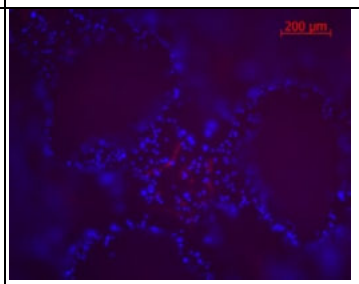	
13	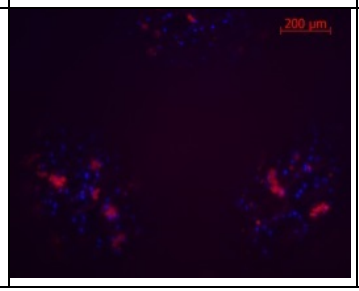	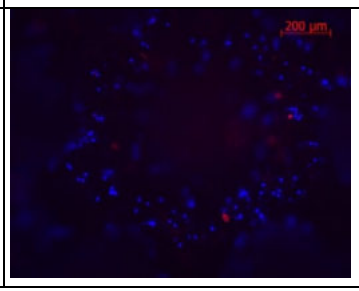	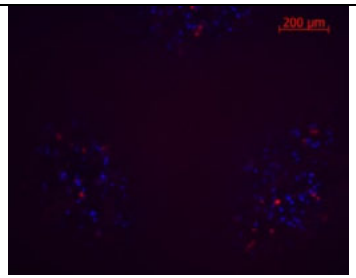	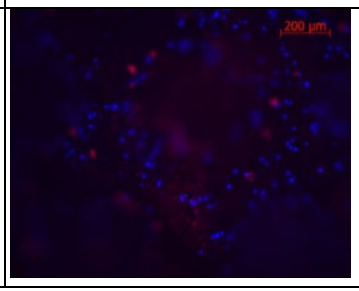	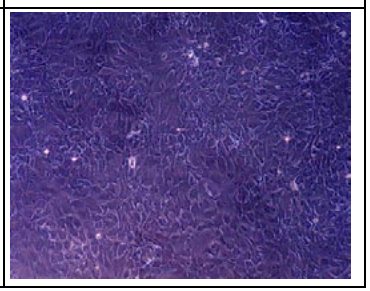

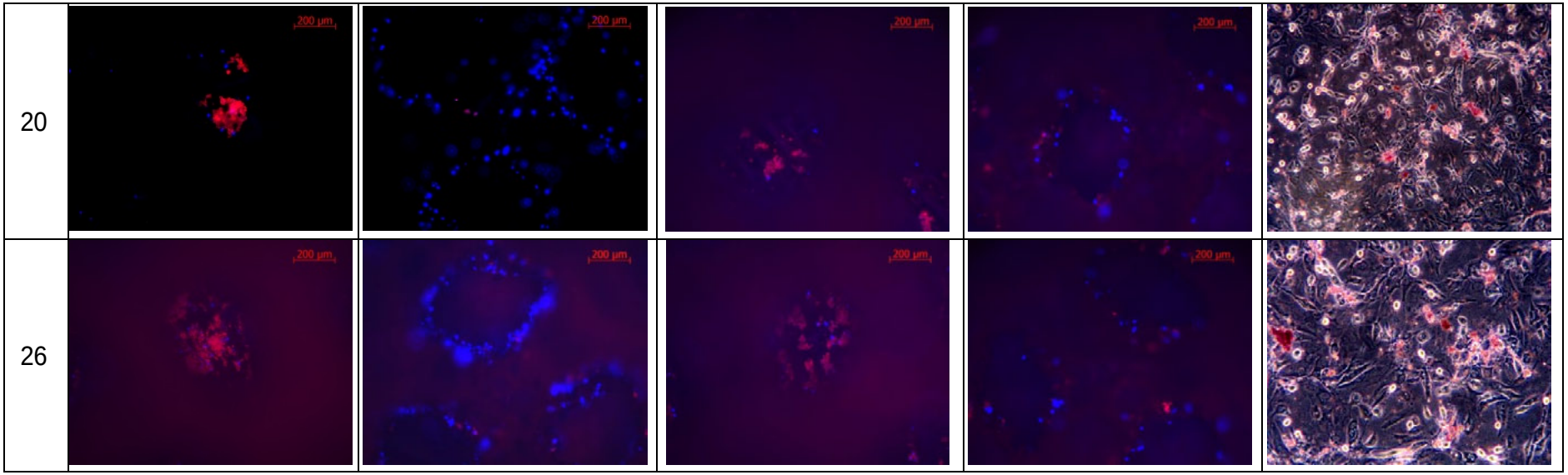

Figure 5.6 Differentiation timeline of rMSCs on untreated Ti64 scaffolds, heat treated Ti64 scaffolds and tissue culture dishes. Cells on untreated and heat treated Ti64 scaffolds were visualised through fluorscence microscopy, and cells on tissue culture dishes were visualised through phase contrast microscopy. Alizarin red stained calcium deposits red. Cell nuclei were counterstained blue with Hoechst

Results seen in Figure 5.6 show the progression of differentiation of rMSCs located on the base and on the struts of untreated and heat treated Ti64 scaffolds, as well as on tissue culture dishes. Alizarin red positive nodules were seen as early as day 13 on both scaffolds substrates, but only at day 20 on the tissue culture dishes. By day 26 it was clear to see that differentiation did occur on both scaffold substrates, and more so than on the tissue culture dishes; from this comparison, one may suggest that the Ti64 material is osteoconducive. This earlier differentiation on the Ti64 is a notable observation, but cannot be firmly concluded as the tissue culture dishes were viewed via different microscopy means. In order to confirm this observation, the test will need to be repeated and cells viewed under the same microscopy conditions. The extent of differentiation was greatest on the base of the untreated Ti64 scaffolds, closely followed by the base of the heat treated Ti64 scaffolds, which agreed with the semi-quantitative analysis results of the 26 day end point experiments. Figure 5.6 also shows the extent of differentiation on the struts of either scaffold substrate to be minimal, independent of cell density.

Once the microscopy of the stained differentiating cells was complete, the cells were harvested to determine their growth rate. This was done to establish whether the cell growth did slow down to allow for differentiation as anticipated. The results from the separate runs were averaged and presented in Figure 5.7.

The doubling time during the cells' growth phase was found to be approximately ten and seven days for the untreated and heat treated Ti64 scaffolds respectively. As anticipated, the doubling time of cells in differentiation medium on untreated and heat treated scaffolds were slower than the three days seen in Figure 5.4 for cells in standard culture medium on both scaffolds substrates. This confirmed that the growth rate of cells did indeed slow down when differentiation occurred on both the scaffold substrates.

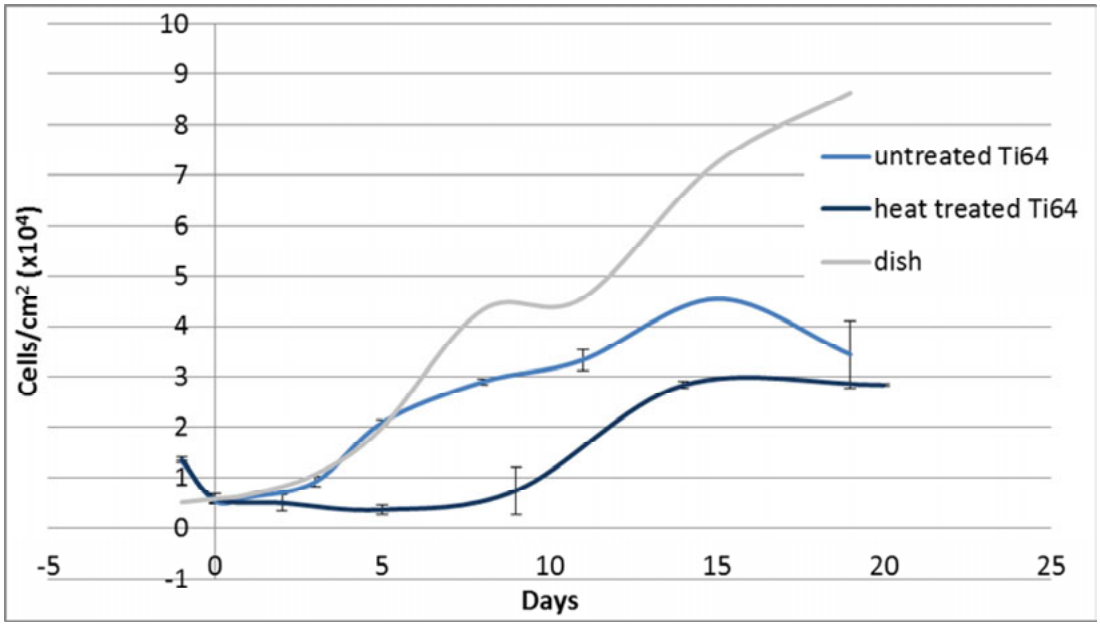

Figure 5.7 Proliferation of rMSCs in differentiation medium on untreated Ti64 (n=4) vs heat treated Ti64 (n=3) scaffolds

In summary, the rMSCs showed differentiation on both the untreated and heat treated Ti64 scaffolds. More differentiation was seen in the untreated scaffolds than in the heat treated scaffolds; as well as more on the base than on the struts of scaffolds. To confirm the differentiation of cells, their growth was measured and shown to be slower than that of cells in standard culture medium.

5.5 Seeding and growth of human MSCs on Ti64 scaffold

Before proceeding with growth and differentiation experiments, it was important to establish the seeding efficiency of human mesenchymal stem cells (hMSCs). Following the same process as described in section 5.2 for the hFibs and the rMSCs, hMSC (passage number 14) were seeded into untreated scaffolds. The results (as seen in Table 5.4) showed a relatively low seeding efficiency of 22% for these cells. This low seeding efficiency was assumed to be due to the manufacturing method of scaffolds, rather than the cells themselves, as the results corresponded with seeding efficiencies obtained on laser sintered substrates in previous studies (Holy *et al.*, 2000; Pfister *et al.*, 2003; Sobral *et al.*, 2011).

Table 5.4 Seeding efficiencies for hMSCs on the untreated (n=5 for P14 cells; n=4 for P6 cells) and heat treated (n=2) experimental Ti64 scaffolds

Cell type	Scaffold type	Seeding no. of cells ($x10^4$)	Remaining no. of cells after 24hours ($x10^4$)	% Seeding efficiency	Average % Seeding Efficiency
Older (P14) hMSCs	untreated	1.4	0.2774	19.81	22.00
		2.53	0.4599	18.18	
		2.53	0.7087	28.01	
		1.39	0.3935	28.31	
		1.5	0.2352	15.68	
Younger (P6) hMSCs	untreated	2.53	0.829	32.77	29.85
		2.53	0.7087	28.01	
		1.36	0.341	25.07	
		1.33	0.446	33.53	
Younger (P6) hMSCs	heat treated	1.889	0.754	39.92	40.02
		2.39	0.959	40.13	

These passage 14 hMSCs were then used to determine the growth and proliferation potential on the untreated Ti64 scaffolds. Growth tests were carried out following the same method and seeding density described for the rMSCs tests. Twenty scaffolds were seeded with duplicate samples and harvested at various time points over three weeks. This test was repeated twice, each time with twenty scaffolds harvested in duplicate at various time points. The results from the four separate runs were averaged and presented in Figure 5.8.

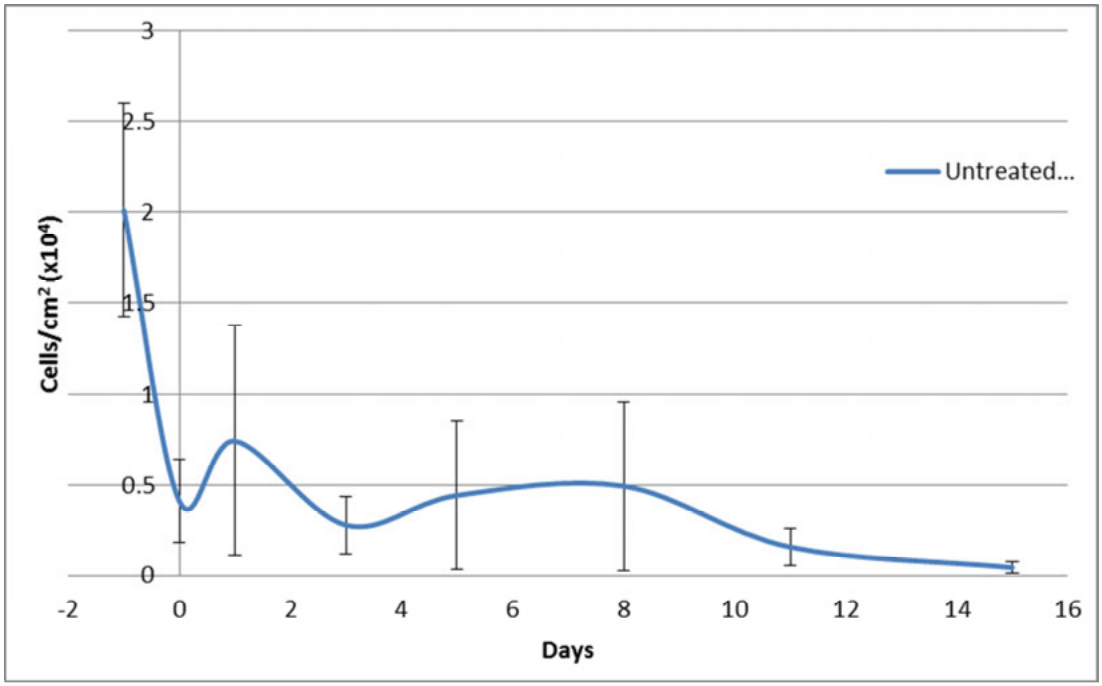

Figure 5.8 Proliferation of older (P14) hMSCs on untreated Ti64 scaffolds (n=4)

From Figure 5.8, one can clearly see that the cells were not proliferating at all, and that almost all the cells had died within two weeks of seeding onto the Ti64 scaffolds. One possible explanation for this cell death was that the cells used were a relatively late passage, and had perhaps reached quiescence or senescence. Therefore, a fresh batch of hMSCs with an earlier passage number (passage number 6) was obtained. These results of the late passage hMSCs highlighted the importance that cell age plays in the success of experiments, which will be discussed further in the next chapter.

Using the passage 6 hMSCs, the seeding efficiency test was repeated on the untreated and heat treated Ti64 scaffolds following the same method previously described. The results shown in Table 5.4 revealed a seeding efficiency of 30% for the cells on the untreated Ti64 scaffolds, and 40% for those on the heat treated Ti64 scaffolds. These results showed a marked improvement in seeding efficiency compared with the later passage hMSCs, and showed the seeding efficiency to be slightly better on the heat treated Ti64 than on the untreated Ti64 scaffolds (Interestingly, the opposite to what was seen on in the rMSC results).

The next set of tests was to determine the growth and proliferative potential of the younger hMSCs on the untreated and the heat treated Ti64 scaffolds. The tests were carried out similarly to that of the rMSCs. The untreated Ti64 scaffold tests were done using sixteen scaffolds harvested in duplicate at eight different time points over three weeks, and then repeated with only eight scaffolds. The results from the two separate runs were averaged and presented in Figure 5.9. The heat treated Ti64 scaffold tests were done using only five scaffolds that were harvested at five different time points over three weeks. The results of this experiment are presented in Figure 5.9. This experiment was not repeated due to the limited number of early passage hMSCs. As with previous experiments, cell growth was measured on standard tissue culture dishes in a parallel experiment as a control.

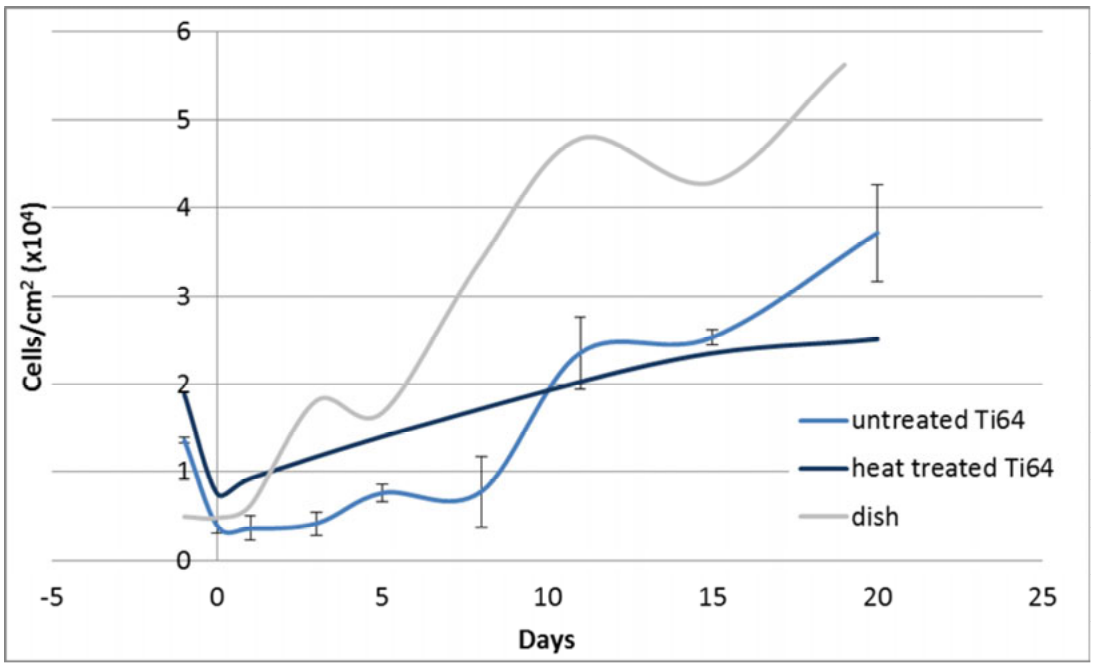

Figure 5.9 Proliferation of hMSCs on untreated Ti64 (n=2), heat treated Ti64 (n=1) and tissue culture dishes (n=1). No statistical analysis was done for growth on heat treated Ti64 scaffolds or on tissue culture dishes

The results of the hMSCs growth on the untreated and heated treated Ti64 scaffolds, and in culture dishes can be seen in Figure 5.9. The doubling time calculated from the cells growth phase for each graph was found to be

approximately three, four, and six for the tissue culture dishes, the untreated Ti64 scaffolds and the heat treated Ti64 scaffolds respectively.

The hMSCs grown on heat treated Ti64 scaffolds appeared to reach a maximum confluency at around day 16, while the growth on the untreated Ti64 did not seem to plateau during the experimental period. The hypothesis earlier posited that cells reached confluence because of limited space on the base of the scaffold also seemed to apply here. The cell nuclei were stained with Hoechst LIVE stain (protocol and concentration in section 4.3.4) and visualised under fluorescence microscopy one day after seeding to observe cell locations within the scaffolds. The results seen in Figure 5.10 show scaffolds, both untreated and heat treated, to have a greater number of cells settled on the base. The number of cells on the struts of the scaffolds appeared to be variable across all experiments done. Considering fewer cells adhere to the struts of the scaffolds, it would be expected for more cells to be adhered to the base and thus for confluency to be reached sooner.

In summary, the hMSCs showed growth on both the untreated Ti64 and the heat treated Ti64 scaffolds. The growth on the heat treated Ti64 scaffolds was slightly more gradual and slower, showing a six day doubling time compared with the four day doubling time of the cells on the untreated Ti64. Finally, the hMSCs were able to adhere to both the base and the struts of both scaffold substrates, however majority of cells settled onto the base of the scaffold, leading to possible early confluency.

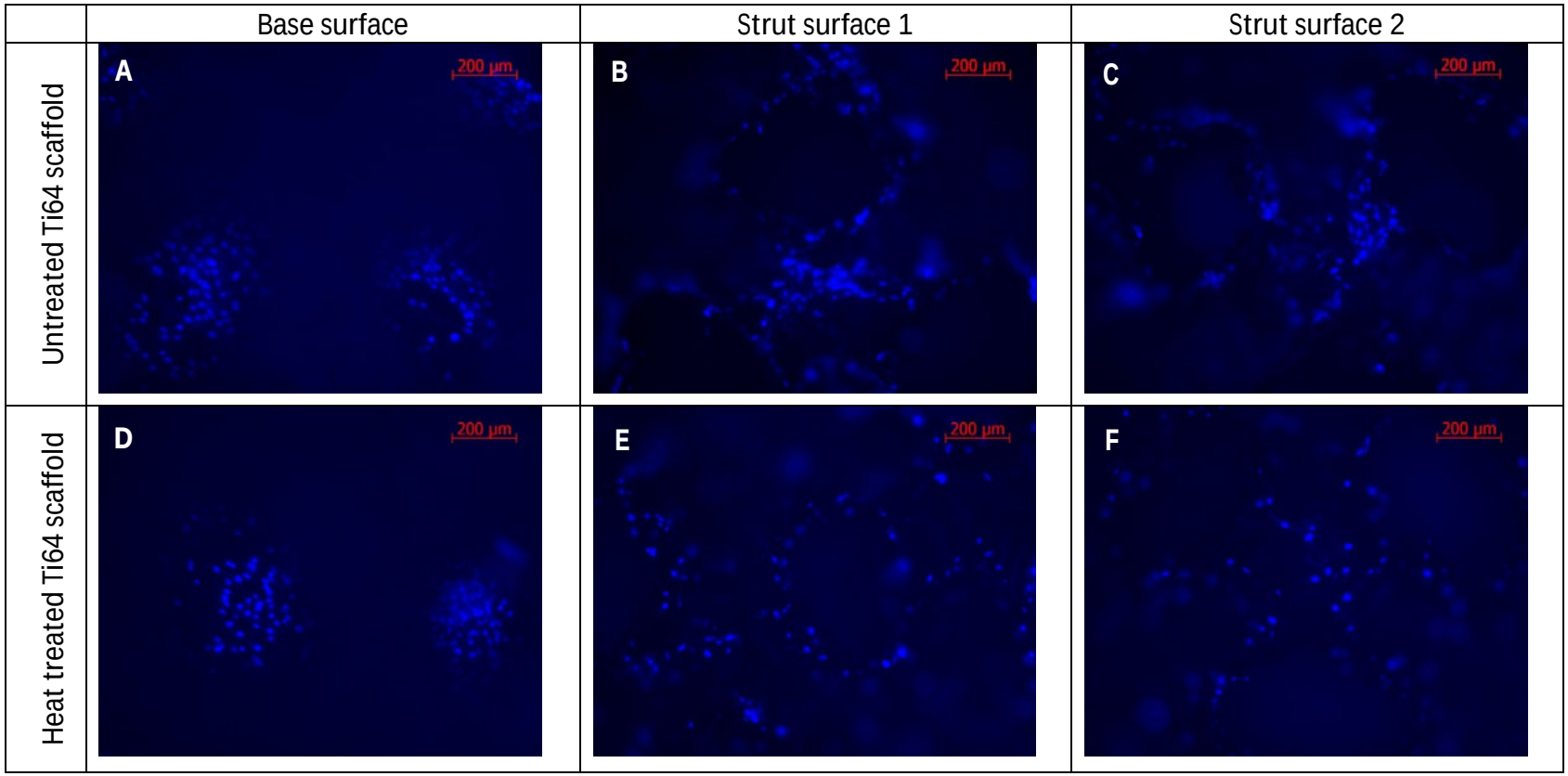

Figure 5.10 Fluorescence microscopy images of human MSCs locations on the Ti64 scaffolds. Cell nuclei have been stained blue with Hoechst LIVE stain. A, B and C represent the hMSCs on the untreated scaffolds. D, E and F represent the hMSCs on the heat treated Ti64 scaffolds. A and D show cells adhered to the base of the scaffolds, where the dark areas of image are out of focus struts. B, C, E and F show cells adhered to the struts

5.6 Differentiation of human MSCs into osteoblasts on Ti64 scaffolds

The final aim was to determine whether the hMSCs were able to differentiate into active osteoblasts and produce bone matrix on the untreated and the heat treated Ti64 scaffolds. These tests were carried out similarly to the differentiation tests done with the rMSCs, firstly establishing the extent of differentiation of the hMSCs with a 26 day endpoint experiment, followed by the three week time-course study of the differentiation.

The 26 day end point study was viewed for calcium deposits using Alizarin LIVE stain to visualise calcium deposits, and Hoechst to visualise cell nuclei (protocol and concentration in section 4.3.4). A semi-quantitative analysis of osteoblast activity was done on five different microscopy images of the base of the scaffolds, as done with the rMSCs. The results for this analysis are shown in Table 5.5, and an example of the images analysed are seen at day 26 in Figure 5.11.

Table 5.5 Semi-quantitative analysis of human osteoblast activity at day 28 on Ti64 scaffolds. (+) denotes, (++) denotes medium and (+++) denotes high

Scaffold	Site no.	No. of nodules	Average	Strength of staining	Average	No. of cells	Average no. of cells
Untreated Ti64	1	+	++	+++	+++	74	68.2
	2	+++		+++		72	
	3	++		++		94	
	4	++		+++		42	
	5	+		++		59	
Heat treated Ti64	1	++	+++	++	+++	70	64.6
	2	+++		+++		72	
	3	+++		+++		52	
	4	+++		+++		76	
	5	++		++		53	

The results in Table 5.5 show that a slightly greater number of calcium nodules were seen on the heat treated Ti64 than on the untreated, even though the strength of staining was equivalent on both the scaffold types. The results also show that there were slightly more cells on the untreated Ti64 than on the heat treated. Considering that there were more calcium nodules seen on the heat treated scaffolds, where there were slightly fewer cells present, it may be suggested that the human MSCs may be more inclined to differentiate into active osteoblasts on the heat treated Ti64 scaffolds. Again, this would however need further testing to confirm.

The following time-course study of the differentiation of the hMSCs was similar to that of the rMSC tests. The untreated Ti64 tests were done by seeding five scaffolds which were stained with Alizarin LIVE and Hoechst LIVE stains for microscopy visualisation, and thereafter harvested at five different time points over three weeks. The heat treated Ti64 tests repeated the untreated Ti64 protocol. The fluorescence microscopy results of both the untreated and heat treated Ti64 scaffolds seen in Figure 5.11 show the progression of differentiation on the scaffolds. The hMSCs were differentiated on standard tissue culture dishes in a parallel experiment as a control. These cells were stained with Alizarin LIVE to view the progression of differentiation using phase contrast microscopy, and the results can be seen in Figure 5.11.

	Untreated Ti64 scaffold		Heat treated Ti64 scaffold		
Day	Base surface	Strut surface	Base surface	Strut surface	Tissue Culture dish
0	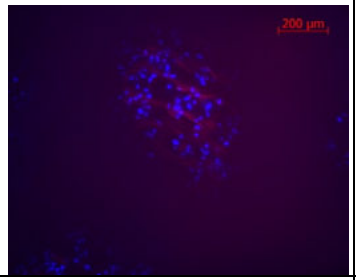	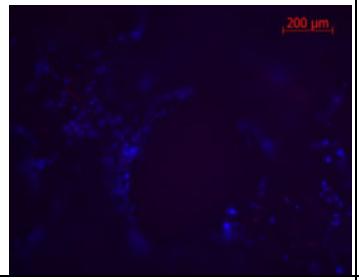	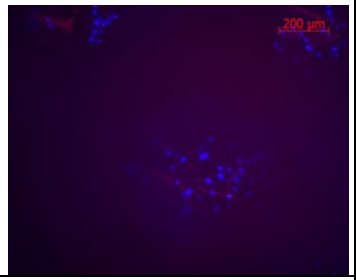	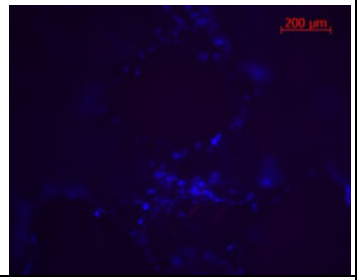	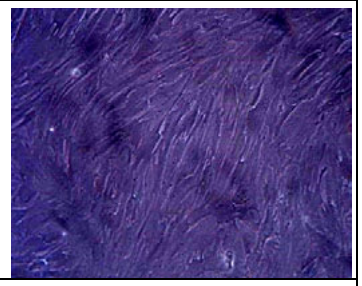
3	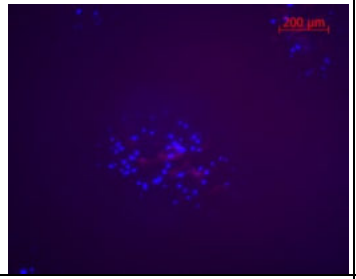	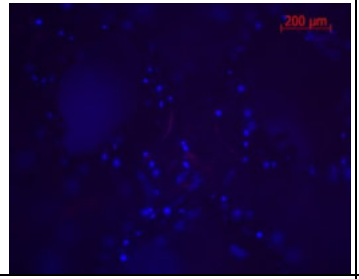	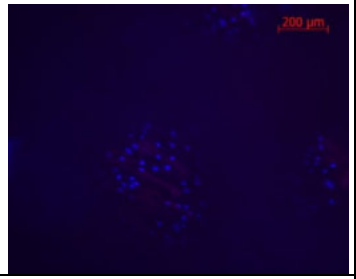	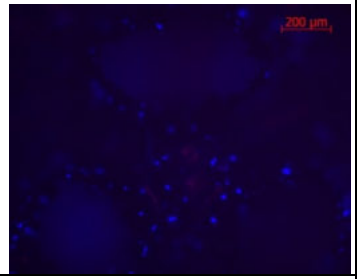	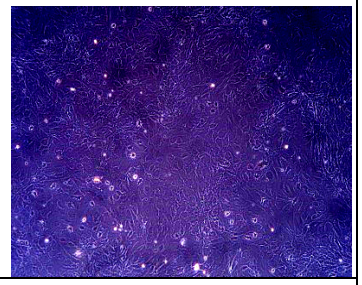
14	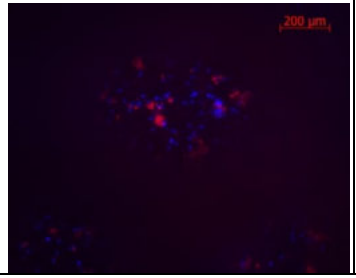	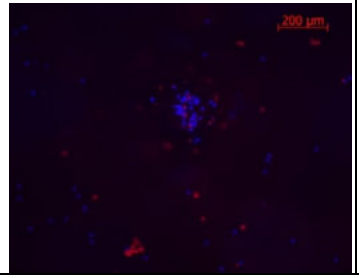	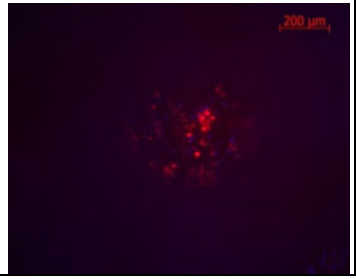	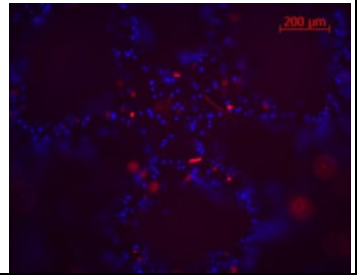	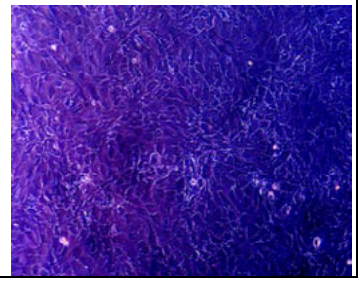

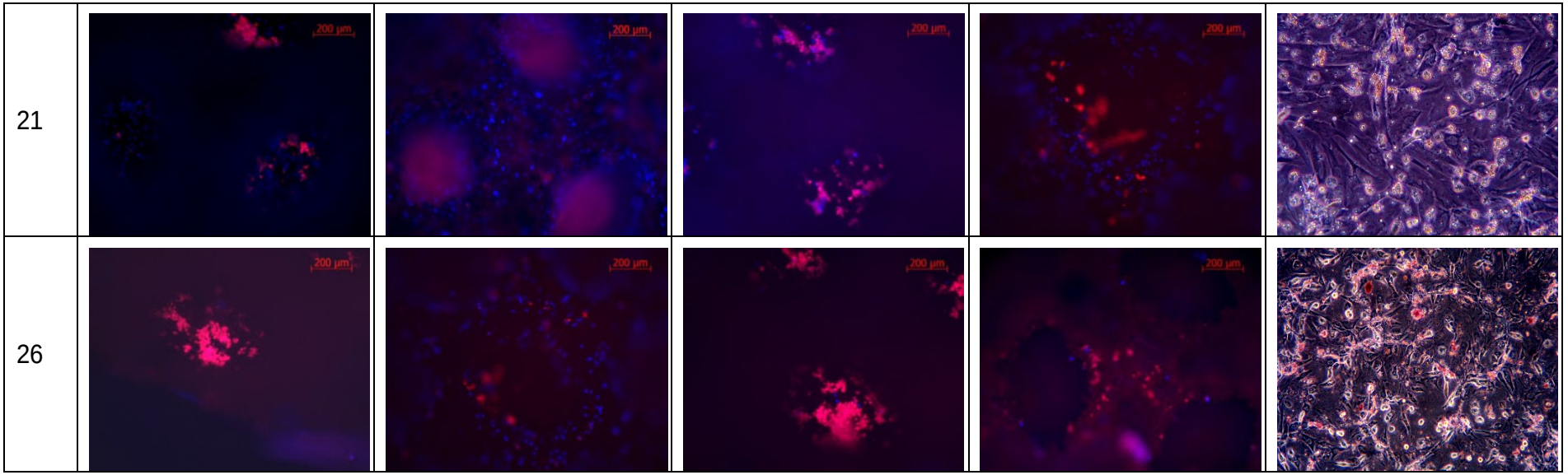

Figure 5.11 Differentiation timeline of hMSCs on untreated Ti64 scaffolds, heat treated Ti64 scaffolds and tissue culture dishes. Cells on untreated and heat treated Ti64 scaffolds were visualised through fluorescence microscopy, and cells on tissue culture dishes were visualised through phase contrast microscopy. Alizarin red stained calcium deposits red. Cell nuclei were counterstained blue with Hoechst

Results seen in Figure 5.11 show the progression of differentiation of hMSCs located on the base and on the struts of untreated and heat treated Ti64 scaffolds, as well as on tissue culture dishes. Alizarin red positive nodules were seen as early as day 14 on both scaffold substrates, but only at day 21 on the tissue culture dishes. By day 26 it was clear to see that differentiation did occur on both scaffold substrates, and more so than on the tissue culture dishes; from this comparison, one may suggest that the heat treated Ti64 material is osteoconducive. However, as with the rMSCs tests, this observation would need to be confirmed by using identical microscopy imaging for both the scaffolds and the tissue culture dishes. The extent of differentiation appeared to be the greatest on the base of the heat treated scaffolds, closely followed by the base of the untreated Ti64 scaffolds, which agreed with the semi-quantitative analysis results of the 26 day end point experiment. Noteably, Figure 5.11 also shows the extent of differentiation on the struts to be far less than that of the base.

Similar to the results seen for the rat MSCs, Figure 5.11 shows Alizarin red positive nodules as early as day 14 on the base and the strut surface on both the original and the heat treated Ti64 scaffolds, and at day 21 on the tissue culture dishes. Differentiation was slightly more abundant on the heat treated Ti64 scaffolds than on the untreated. A notable difference was seen between the amount of differentiation occurring on the base and on the struts of both scaffold types, as minimal differentiation was seen on the struts.

Once the microscopy of the stained differentiating cells was complete, the cells were harvested to determine their growth rate. This was done to establish whether the cell growth did slow down when differentiation occurred as anticipated. The results for the growth rate of cells in differentiation medium are presented in Figure 5.12.

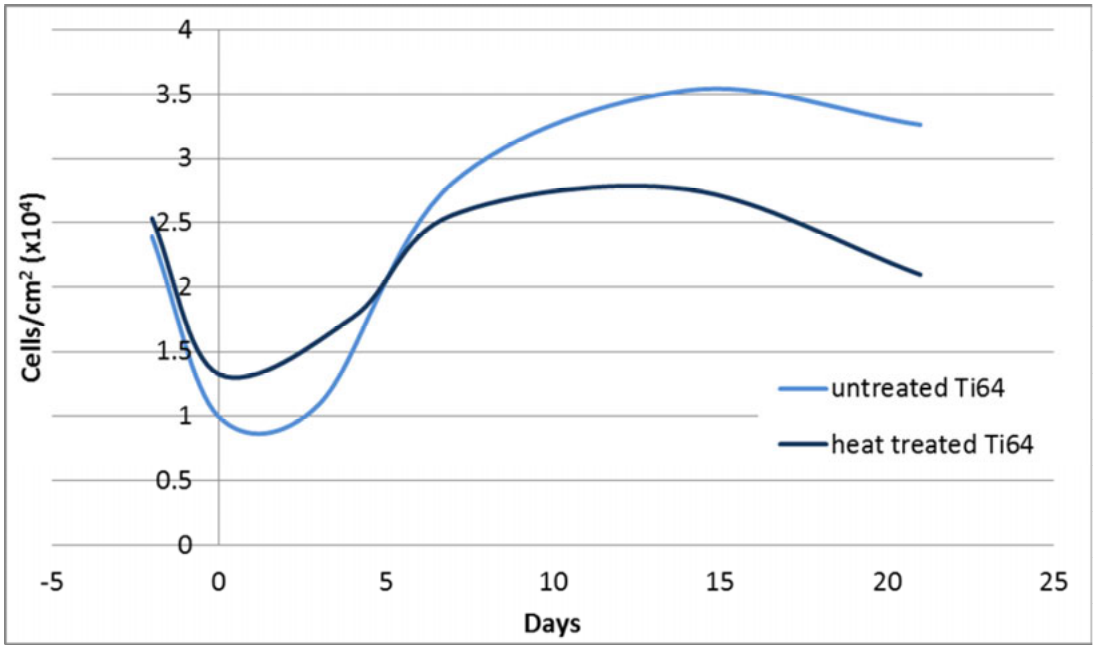

Figure 5.12 Proliferation of hMSCs in differentiation medium on original Ti64 (n=1) vs TO Ti64 (n=1) scaffolds

The doubling time was found to be approximately six and seven days for the untreated and heat treated Ti64 scaffolds respectively. As anticipated, the doubling time of cells in differentiation medium on untreated and heat treated scaffolds were slower than the four and six days seen in Figure 5.9 for cells in standard culture medium on respective scaffolds. This confirmed that, although minimally, the growth rate of cells did indeed slow down to allow for differentiation on both the scaffold substrates. The slower doubling time calculated for the differentiating cells on the heat treated scaffolds, compared to that of the untreated Ti64 scaffolds substantiates the greater extent of differentiation seen on the same substrate in the microscopy images and semi-quantitative analysis.

In summary, the hMSCs showed differentiation on both the untreated and heat treated Ti64 scaffolds. More differentiation was seen in the heat treated scaffolds than in the untreated scaffolds; as well as more on the base than on the struts of scaffolds. To confirm the differentiation of cells, their growth was measured and shown to be slower than that of cells in standard culture medium.

6 Discussion

As the number of joint replacement surgeries rise, so do the number of revision surgeries done to replace or repair existing artificial joints, with aseptic loosening being the leading cause (Kurtz *et al*., 2007; National Joint Registry, 2012). Aseptic loosening of the joint occurs through the mechanical and biological loss of implant fixation to the bone. As the joint begins to mechanically deteriorate, debris particles are released into the surrounding tissues resulting in inflammation, macrophage invasion and osteolysis, and thus biological deterioration. By implementing a three dimensional porous structure at the bone-implant interface, a stronger three dimensional interlocking of the bone and implant might be possible. This would also play an important structural role of the implant by reducing the possibility of stress shielding and shearing at the interface. In this study, it is hypothesized that the seeding of the three dimensional scaffolding structure with mesenchymal stem cells will improve the potential for osseointegration of the implants, as the existing bone may be more inclined to unite with developing bone from the differentiating MSCs than with the implant substrate.

To further improve the implants against failure, heat treatment of the implant material, Ti64, has previously been seen to vastly improve the strength as well as reduce the debris formation to nearly zero (Allen, Bloycet, & Bell, 1996; Mudd, Vicatos, & Basson, 2003). The question of how this heat treatment will affect the MSCs capabilities and potential osseointegration then arises. In order to fully prove the hypothesis that the pre-seeding of scaffolds with MSCs will improve the osseointegration of implants, *in vivo* tests will need to be done once the effects of heat treatment have been concluded. The purpose of this study was thus to investigate the effects that the thermal oxidisation, or heat treatment process of the Ti64 scaffolds would have on the potential capabilities of the seeded mesenchymal stem cells *in vitro*.

Previous studies have shown the effects that Ti64 heat treatment has on the initial seeding of cells (García-Alonso *et al*., 2003), and the short term growth and

differentiation (seven days) (Saldaña *et al*., 2005) on flat Ti64 samples; however no studies have been found looking at survival, growth and differentiation of cells on a three dimensional scaffold. The findings in this study show that the heat treatment of the Ti64 does not have a considerable effect on the cells ability to proliferate and differentiate into osteoblasts. This was shown through the assessment of cell adhesion, growth and differentiation on untreated Ti64 compared with that on the heat treated Ti64. What was importantly noted was that the location of the cells within the three dimensional scaffolds had an important contributing factor on the cells' performance.

6.1 Untreated vs heat treated Ti64 cell work

To assess the effect the heat treatment of Ti64 on the adherence of mesenchymal stem cells, the cells were seeded onto both the untreated and heat treated Ti64 scaffolds for comparison. The heat treatment was seen to make minimal difference to the number of adhering cells. For both the rat and the human MSCs test results, seen in chapter 5, the adherence of cells was within 10% of one another for the untreated and heat treated Ti64. This agreed with the results García-Alonso *et al*. (2003) found when testing the adhesion properties of human osteoblastic cells on untreated and heat treated Ti64 samples. Their study reported no significant difference in the number of attached cells on the untreated and the heat treated Ti64 surface at all inspected time points over a 24 hour period shown in Figure 6.1.

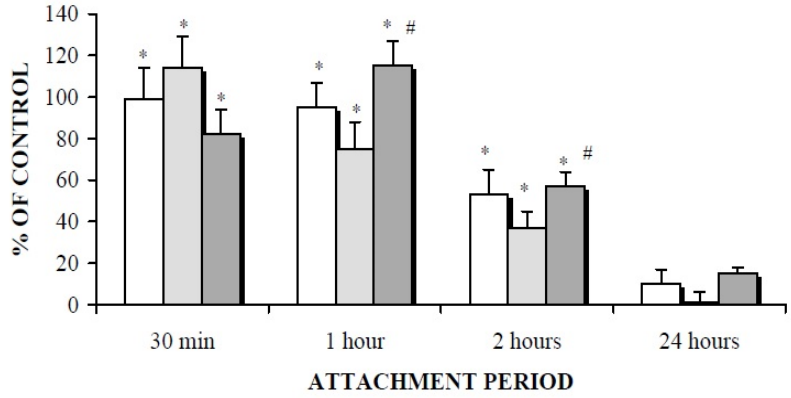

Fig. 8. Osteoblasts attachment on different substrates: PS (Control) (□), polished untreated Ti64 (■), Ti64 500 (▢), Ti64 700 (▢). Cell attachment under standard cell culture conditions was determined at 30 min, 1, 2 and 24 h. The attached osteoblasts labelled with BCECF-AM were quantified by spectrofluorimetry. The results indicate the percentage of osteoblast attached to Ti64, Ti64 500 and Ti64 700 in relation to PS control. Results are mean ± SE. $n = 6$. (*) $p < 0.001$: Control vs. Ti64, Ti64 500 and Ti64 700 in all time matched values. (#) $p < 0.05$: Ti64 500 vs. Ti64 700 at 1 and 2 h.

Figure 6.1 Results from García-Alonso *et al.*'s (2003) study showing cell adhesion on control dishes, untreated and heat treated Ti64 substrates over a24 hours period

The next step was to assess the effect the heat treatment of Ti64 on the growth of the MSCs. The doubling times of the rat and the human MSCs appeared to be slightly longer on the heat treated Ti64, suggesting that the treatment possibly does marginally slow the rate of cell growth. However, the results presented by Saldaña *et al*. (2005) suggest that heat treatment of Ti64 substrate does not affect the cell growth. Saldaña *et al*. (2005) cultured human primary bone cells on untreated and heat treated (at 500 °C and 700 °C) Ti64 disks in standard culture medium for up to seven days. Their results showed a much faster overall growth of cells on both substrates, with no noteworthy change in cellular growth on either heat treated Ti64 substrate. The possible differences in growth results for the different Ti64 substrates seen in this study and those seen in Saldaña *et al*.'s (2005) study may be explained by a few reasons:

- The cells used by Saldaña *et al*. (2005) were primary bone cells harvested from bone, which may possess different growth properties to that of mesenchymal

stem cells harvested from adipose tissue. The subject of cell source and cell age will be discussed further in section 6.3.

- This study cultured cells on 3D Ti64 scaffolds, whereas Saldaña *et al*.'s (2005) study was carried out on flat Ti64 disks. This would suggest that the location of cells may affect the cells growth which will be discussed further in section 6.2.

The final characteristic to assess the effects heat treatment of Ti64 would have on was the differentiation of MSCs. The imaging results of differentiation, seen in Figure 5.6 and Figure 5.11, show similar timelines of differentiation occurring on both the untreated and heat treated Ti64 for both the rat and the human cells. Semi-quantitative image analysis was used in this study as it was suffice to determine the extent of differentiation for the purpose of this study. If one needed further analysis in future applications, full quantitative image analysis may be done. The semi-quantitative analysis of differentiation images, showed the extent of differentiation to be slightly higher for the rat MSCs on the untreated Ti64, and slightly higher on the heat treated scaffolds for the human MSCs. The semi-quantitative results obtained for the human cells showing slightly more differentiation occurring on the heat treated Ti64 over 26 days aligns with the work done by Saldaña *et al*. (2005). Saldaña *et al*. (2005) measured the levels of differentiation markers such as alkaline phosphatase activity, osteocalcin, and osteoprotegerin after only two days in differentiation medium, for human osteoblasts on untreated Ti64 and 500 °C heat treated and 700 °C heat treated Ti64. For all three markers, the expression or activity levels were higher on the heat treated Ti64 than the untreated Ti64. The visual extent of mineralized nodules was also seen to be greater in the heat treated Ti64. Their work concluded that the heat treatment, using either temperature, would improve the biocompatibility of the Ti64. Semi-quantitative image analysis was used in this study as it was suffice to determine the extent of differentiation for the purpose of this study. If one needed further analysis in future applications, full quantitative image analysis may be done.

Nishiguchi *et al*. (2001; 2003) repeatedly showed the improved rate and extent of bone formation on alkali and heat treated Ti64 compared to that of untreated Ti64 *in vivo*. Their tests assess the extent of bone attachment after implantation for 12 weeks in the femur bone of beagle dogs, with the results showing significant differences between the different substrates. Their work proposed that the alkali and heat treatments of Ti64 made the substrate osteoconducive. This would explain the greater saturation of bone matrix seen on the heat treated Ti64 in the human MSC tests in this study, as well as the improved biocompatibility of heat treated Ti64 seen by Saldaña *et al*. (2005).

6.2 Location of cells on the scaffolds

It was interesting and unexpected to note in this study that the location of the cells within the scaffolds played an important role on the outcome of the functioning of the cells. This was initially noted when microscopy images were taken to view possible reasons for the low seeding efficiencies of between 30-40%. For both the rat and the human MSCs tests, and on both the untreated and heat treated Ti64 scaffolds, a greater number of cells were seen to have adhered to the base of the scaffolds as opposed to the struts. Holy *et al*. (2000) suggest that the cell size is so miniscule compared with the scaffold pores defined by the struts, and developed by the rapid prototyping process, that the cells penetrate through and accumulate at the bottom of the scaffold. Sobral *et al*. (2011) point out that pore structure and size play an important role in cell migration and adhesion. Their work showed that a pore size of 100 µm retained approximately 10% more cells in the scaffolds than those with 750 µm sized pores. Furthermore, when using a gradient pore size from 750-100 µm with the smallest pore size being in the centre of the depth of the scaffold, 35% more cells were retained than those on scaffolds with only 100 µm pore sizes. The scaffolds in this study were designed to have a pore size of 500 µm, thus it may be suggested that it is highly likely that the cells would pass through the pores and accumulate at on the base of the scaffolds, which is what the imaging results showed. The low seeding efficiency is also likely due to cells flowing out of

the scaffold structure entirely and into the containing dishes when flooded with culture medium after seeding, because of the pore size being non-restrictive.

The location of cells has already been shown to affect the growth of the cells in sections 5.3 and 5.5. As the pore size of the scaffold was non-restrictive to the cells movement, majority of cells were able to settle on the base of the Ti64. Cells were then able to reach confluency and plateau earlier than if they were more sparsely seeded. Correspondingly, it was interesting to note in Figure 5.6 and Figure 5.11 that the sparsely seeded struts of the scaffolds were reluctant to differentiate and rather remained as mesenchymal stem cells. This was possibly related to the cell density on the struts, as one can see in Figure 5.11 that where the cells density is greater, differentiation does start occurring on the struts. Another possible explanation for the lack of differentiation on the scaffold struts is the role that initial cell attachment has on potential proliferation and differentiation. The reorganization of the cytoskeleton at contact interfaces during attachment result in morphological and behavioural changes in the cell that have lasting effects on the cells growth and differentiation capabilities (Gwynn, 1994). This may suggest that the morphology that the cells adhered to the struts assume, may be non-conducive to differentiation, again highlighting the importance of cell location within the scaffolds.

The contributing factor of the cells location in the scaffold is important when considering the clinical application of these scaffolds. In order to obtain better cell seeding on the struts of the scaffold, one may consider seeding cells in a rolling culture environment. This is when the culture is continuously revolved to negate the effects of gravity. This situation would avoid the gravitational settling of cells through the pores onto the base, allowing more cells to settle on the struts. However, one would need to first consider and research further whether cells seeded on the struts are important for application. This would be understood in *in vivo* studies to determine if the host bone growth into the pores unites with developing bone on the base of scaffolds well enough to render the struts a three

dimensional interlocking mechanism rather than a bonding site. If this is the case, the struts would become saturated with bone and show the same fixation results.

6.3 Technical difficulties

The greatest challenge faced in this study was the difficulty culturing the human mesenchymal stem cells. The age (passage number) of the cells, as well as their tissue source play an important role in the success in *in vitro* work. Kern, Eichler, Stoeve, Klüter, & Bieback (2006) and Sakaguchi, Sekiya, Yagishita, & Muneta (2005) compared the *in vitro* proliferation and differentiation potential of various tissue sourced MSCs. Kern *et al*. (2006) showed that human MSCs were found in highest concentration in adipose tissue (AT), and that AT derived cells showed no significant difference in their osteogenic differentiation potential compared with bone marrow (BM) derived MSCs, making them an attractive source for MSCs. Sakaguchi *et al*. (2005) however reported that although MSCs were able to differentiate into various lineages, BM derived MSCs still showed the highest levels of osteogenesis, and AT derived MSCs showed the highest levels of adipogenesis. Although the hMSCs used in this study were AT derived, which may not show the maximal osteogenic differentiation, the culturing difficulties appear to be more from the passage number (age) of the cells than their tissue source.

Kern *et al*.'s (2006) work showed that the MSCs have a limited proliferation capacity in that as the cells age, the *in vitro* doubling time of cells is hindered. For AT derived MSCs, they reached proliferative senescence after passage seven. Sakaguchi *et al*. (2005) also reported the slower doubling time of MSCs the longer they remained in culture; however, they noted that although the doubling time was slower, the BM derived MSCs retained proliferative ability up to the tenth passage, whereas AT derived MSCs lost theirs at the eighth passage. Bonab *et al*. (2006) supported this by showing that at later stages of *in vitro* culturing of MSCs, the cells became rounded, vacuolated and detached from the base of the culture flask. As the human cells in this study that showed poor growth and continuously detached from Ti64 scaffolds after two weeks in culture, were of a late passage (P14), they appear to

conform to the results seen in these previous studies. Considering these previous results, the passage 6 human cells used in this study may also show adhesion and proliferation that is lessened than the potential of younger cells to be used in future applications.

Finally, Stenderup, Justesen, Clausen, & Kassem (2003) pointed out that not only is the *in vitro* aging of the cells important when considering the effects on cell proliferation, but also the age of the patient. They reported that for MSCs obtained from patients 66 years and older, the cell maximal life span, and the rate of proliferation were greatly reduced compared with MSCs obtained from patients between the age of 18 and 29 years. Although the patient age, combined with the length of time in culture had huge effects on the proliferation capabilities of the cells, it did not appear to affect the differentiation capabilities. The reduced presence of osteogenesis is thus due to the reduced presence of viable cells rather than the lack of differentiation of cells.

In summary, the patient's age and the aging of cells during *in vitro* culture greatly affect the proliferative capacities of the MSCs. The tissue source of the MSCs showed differentiation potential into any of the mesenchymal lineages; however MSCs were more inclined to differentiate into cells associated with the tissue they were derived from. These are important factors to note, as the patients intended for this therapy for joint replacements are likely to be older, thus possibly requiring higher volumes of MSCs and shorter term *in vitro* culturing for therapies to be effective.

7 Conclusions

Based on the preceding information presented in this study, the following conclusions are able to be drawn:

7.1 Heat treatment of Ti64 does not adversely affect the cells capabilities

None of the results obtained on the heat treated Ti64 were considered notably different to those seen on the untreated Ti64. The seeding efficiency of cells on both substrates were within 10% of one another for both the rat and the human MSC experiments. The growth of cells on the heat treated Ti64 was seen to be slightly slower than that on the untreated, but not considerably so. This slight variance in cell growth may also be due to the other contributing factors outlined in section 6.1. Lastly, the extent of differentiation was similar on both substrates, but slightly greater on the untreated Ti64 for the rat MSC tests, and on the heat treated Ti64 for the human MSC tests. The results of the human tests are substantiated by other reports detailed in section 6.1. Importantly, the results show that heat treatment of Ti64 does not adversely affect the cells survival, growth and differentiation. This suggests that identical therapies may be implemented on the heat treated Ti64 as on the untreated, thus taking advantage of the added mechanical benefits the heat treatment offers.

7.2 Ti64 may be considered an osteoconducive material

Figure 5.6 and Figure 5.11 showed the first deposits of calcium nodules at day 13 and 14 of the rat and human MSC differentiation experiments respectively. The differentiation of the human MSCs, which was supported by various other reports, showed a greater extent of differentiation of the heat treatment Ti64. From this result, one is able to suggest that the heat treated Ti64 substrates are osteoconducive. This conclusion was supported by work done by Li *et al*. (2007), García-Alonso *et al*. (2003), Saldaña *et al*. (2005) and Nishiguchi *et al*. (2001; 2003).

7.3 Cell proliferation and differentiation are sensitive to cell source and age of donor

Mesenchymal stem cells have the capability to differentiate into all mesenchymal lineage tissues. It has however been shown that cells from particular areas may be more inclined to differentiate into certain terminal cells. For example, MSCs found in bone marrow may be more likely to differentiate into osteoblasts, whereas MSCs found in adipose tissue may be more likely to differentiate into adipocytes. This by no means suggests that certain MSCs should be disregarded for use if not derived from the desired tissues; it would just need to be considered for the timeframe for expansion and differentiation of cells, depending on patient factors.

Patient factors such as age need to be considered when harvesting MSCs for therapeutic uses. MSCs from older patients are less likely to proliferate as quickly as those from younger patients, yet their differentiation capabilities are unaffected. The same applies for cell aging during *in vitro* expansion. The longer cells are cultured *in vitro*, the less proliferative they become, eventually rounding up and detaching from the culture substrate completely. Derived MSCs should be cultured *in vitro* for as little time as possible to avoid altering of cells and reduced viability.

7.4 Cell differentiation is also dependent on cell's location in the scaffolds

The functioning of the rat and the human MSC were dependent on the location of the cells within the scaffold. This is understood when examining the adherence and growth of cells on the base of the scaffolds versus the struts. As well as considering the extent of differentiation of cells on the base versus the struts of the scaffolds. A large difference in the number of cells was seen to have settled on the base compared with the struts; cells were also more inclined to differentiate on the base than on the struts. This is important to note for further *in vivo* studies to determine if the struts are a primary bonding site or rather a three dimensional interlocking mechanism.

8 Future recommendations

Based on the above conclusions, the following recommendations are made for future work:

8.1 Research methods to consistently seed struts of scaffolds

As the seeding of scaffolds across all experiments in this study showed inconsistent number of cells on the struts of the scaffolds, one would need to test and develop a method to seed cells onto the base while obtaining a consistent number of cells on the struts. This would allow for the full surface area to be utilised for cell attachment, thus allowing more area for cell proliferation. A possible method of doing this would be to seed and grow cells in a "rolling" culture where the culture and scaffolds are continuously rotated to prevent gravity being the determine factor of cell settling. This would be a good way to allow more cells to adhere to the struts of the scaffolds, as well as angled surfaces. By generating consistently seeding results, one would be able to better determine the extent of growth and differentiation on the struts as well as on the scaffold as an entirety.

8.2 MSC versus osteoblast adherence and success on scaffolds

This study reported the adherence of MSCs, which were then allowed to proliferate and differentiate on the Ti64 scaffolds. Many previous reports show results for the adherence of osteoblasts or preosteoblasts, which are then allowed to differentiate on the Ti64 scaffolds (Boyan *et al.*, 2001; García-Alonso *et al.*, 2003; Saldaña *et al.*, 2005; Sobral *et al.*, 2011; Yang *et al.*, 2002). Considering these scaffolds have the potential of being implanted, they would likely encounter a mixed population of mesenchymal and osteoblastic cells. It would be of use to test the adherence and subsequently the differentiation and matrix deposition of MSCs and osteoblasts separately, and then collectively. This would be able to show what cell population, or mix thereof, would best be suited for the *in vivo* therapy.

8.3 *In vivo* tests of the osseointegration of the scaffolds

Finally, before this therapy would be able to be implemented, one would need to do extensive *in vivo* studies to observe any unexpected effects. *In vivo* tests would need to show whether the seeding of scaffolds prior to implantation does in fact improve osseointegration by allowing a more natural union of host bone ingrowth to the seeded developing bone cells as suggested at the beginning of this report; or if the heat treatment of the Ti64 alone would osteoconducive enough to form the strong bonding of bone to the implant. The function of the struts would also need to be fully determine by *in vivo* studies, to understand if they are primarily a bone union site or rather a three dimensional interlocking mechanism.

9 References

Abu-Amer, Y., Darwech, I., & Clohisy, J. C. (2007). Aseptic loosening of total joint replacements: mechanisms underlying osteolysis and potential therapies. *Arthritis research & therapy*, *9 Suppl 1*, S6. doi:10.1186/ar2170

Allen, C., Bloycet, A., & Bell, T. (1996). Sliding wear behaviour of ion implanted ultra high molecular weight polyethylene against a surface modified titanium alloy Ti-6Al-4V. *Tribology International*, *29*(6), 527–534.

Anchorage, D. B. (1981). Osseointegrated titanium implants. *Acta orthopaedica*, *52*, 155–170.

Anderson, J. M. (2001). Biological Responses to materials. *Annual Review of Materials Research*, *31*, 81–110.

Anselme, K., Linez, P., Bigerelle, M., Le Maguer, D., Le Maguer, a, Hardouin, P., … Leroy, J. M. (2000). The relative influence of the topography and chemistry of TiAl6V4 surfaces on osteoblastic cell behaviour. *Biomaterials*, *21*(15), 1567–77. Retrieved from http://www.ncbi.nlm.nih.gov/pubmed/10885729

ASTM International. Standard specification for Wrought 18chromium-14nickel-2.5molybdenum stainless steel bar and wire for surgical implants (2003). West Conshohocken.

ASTM International. Standard specification for unalloyed titanium, for surgical applications (2006). West Conshohocken.

ASTM International. Standard specification for Wrought Colbalt-20Chromium-15Tungsten-10Nickel alloy for surgical implant applications (2007). West Conshohocken.

ASTM International. Standard specification for wriught Titanium-6Aluminium-4Vanadium ELI (Extra low interstitial) alloy for surgical implant applications (2008). West Conshohocken.

ATCC. (2011). Adipose-derived mesenchymal stem cells: Normal, Human. Retrieved from www.atcc.org/~/ps/PCS-500-011.ashx

ATCC. (2012). *ATCC ® Stem Cell Culture Guide tips and techniques for culturing stem cells*. Retrieved from https://www.atcc.org/~/media/PDFs/Culture Guides/iPSCguide.pdf

Baba, S., Inoue, T., Hashimoto, Y., Kimura, D., Ueda, M., Sakai, K., … Hojo, M. (2010). Effectiveness of scaffolds with pre-seeded mesenchymal stem cells in bone regeneration —Assessment of osteogenic ability of scaffolds implanted under the periosteum of the cranial bone of rats—. *Dental Materials Journal*, *29*(6), 673–681. doi:10.4012/dmj.2009-123

Bacabac, R. G., & Mullender, M. G. (2005). [Mechanobiology of bone tissue] Mecanobiologie du tissu osseux. *Pathologie Biologie*, *53*, 576–580. doi:10.1016/j.patbio.2004.12.005

Barrere, F., van der Valk, C., Meijer, G., Dalmeijer, R., de Groot, K., & Layrolle, P. (2003). Osteointegration of biomimetic apatite coating applied onto dense and porous metal implants in femurs of goats. *Journal of Biomedical materials research Part B: Applied Biomaterials*, *67*, 655–665.

Becker, T., & Vicatos, G. (2005). *Comparative study of fatigue performance of SLS and commercially available rolled and annealed titanium material*. University of Cape Town.

Bonab, M. M., Alimoghaddam, K., Talebian, F., Ghaffari, S. H., Ghavamzadeh, A., & Nikbin, B. (2006). Aging of mesenchymal stem cell in vitro. *BioMed Central cell biology*, *7*(14). doi:10.1186/1471-2121-7-14

Boyan, B. D., Lohmann, C. H., Dean, D. D., Sylvia, V. L., Cochran, D. L., & Schwartz, Z. (2001). Mechanisms involved in osteoblast response to implant surface morphology. *Annual Review of Materials Research*, *31*, 357–371.

Bracken, W., Sharma, R., & Elsner, Y. (1985). Vanadium accumulation and subcellular distribustion in relation to vanadate induce cytotoxicity in vitro. *Cell Biology and Toxicology*, *1*(4), 259.

Brodbeck, W. G., & Anderson, J. M. (2009). Giant cell formation and function. *Current Opinion in hematology*, *16*(1), 53–57. doi:10.1097/MOH.0b013e32831ac52e.GIANT

Creese, R. (1999). *Introduction to Manufacturing Processes and Materials* (1st ed.). New York: Marcel Dekker, Inc.

Dabrowski, B., Swieszkowski, W., Godlinski, D., & Kurzydlowski, K. (2010). Highly porous titanium scaffolds for for orthopaedic applications. *Journal*

of biomedical materials research Part B: Applied biomaterials, *95B*, 53–61.

Dario-Becker, J. (2012). *Derived copy of biology: Mixed majors, Part 2*. Connexions web site. Retrieved from http://www.cnx.org/content/col11592/1.2

Davies, J. E. (2003). Understanding Peri-Implant Endosseous Healing. *Journal of Dental Education*, *67*(8), 932–949.

Díaz, C., Lutz, J., Mändl, S., García, J. a., Martínez, R., Rodríguez, R. J., … Conde, a. (2008). Comparison of tribological behaviour and biocompatibility of Ti6Al4V alloy after ion implantation or thermal oxidation. *Physica Status Solidi (C)*, *5*(4), 947–951. doi:10.1002/pssc.200778310

Engler, A. J., Sen, S., Sweeney, H. L., & Discher, D. E. (2006). Matrix elasticity directs stem cell lineage specification. *Cell*, *126*(4), 677–89. doi:10.1016/j.cell.2006.06.044

Freeman, M. (1976). *Engineering in medicine, volume 2. Artificial hip and knee joint technology*. (M. Schaldach & D. Hohmann, Eds.) (pp. 127–137). Berlin Heidelberg: Springer Berlin Heidelberg.

Frosch, K.-H., & Stürmer, K. M. (2006). Metallic Biomaterials in Skeletal Repair. *European Journal of Trauma*, *32*(2), 149–159. doi:10.1007/s00068-006-6041-1

Gandhi, R., Tsvetkov, D., Davey, J. R., & Mahomed, N. N. (2009). Survival and clinical function of cemented and uncemented prostheses in total knee replacement: a meta-analysis. *The Journal of bone and joint surgery. British volume*, *91*(7), 889–95. doi:10.1302/0301-620X.91B7.21702

García-Alonso, M. C., Saldaña, L., Vallés, G., González-Carrasco, J. L., González-Cabrero, J., Martínez, M. E., … Munuera, L. (2003). In vitro corrosion behaviour and osteoblast response of thermally oxidised Ti6Al4V alloy. *Biomaterials*, *24*(1), 19–26. Retrieved from http://www.ncbi.nlm.nih.gov/pubmed/12417174

Geurs, N., Jeffcoat, R., McGlumphy, E., Reddy, M., & Jeffcoat, M. (2002). Influence of implant geometry and surface characteristics on progressive osseointegration. *The international journal of oral and maxillofacial implants*, *17*, 811–815.

Guleryuz, H., & Cimenoglu, H. (2005). Surface modification of a Ti–6Al–4V alloy by thermal oxidation. *Surface and Coatings Technology*, *192*(2-3), 164–170. doi:10.1016/j.surfcoat.2004.05.018

Gwynn, I. (1994). Cell biology at interfaces. *Journal of Materials Science: Materials in Medicine*, *5*(6-7), 357–360.

Haleem-Smith, H., Argintar, E., Bush, C., Hampton, D., Postma, W. F., Chen, F. H., … Tuan, R. S. (2012). Biological responses of human mesenchymal stem cells to titanium wear debris particles. *Journal of orthopaedic research : official publication of the Orthopaedic Research Society*, *30*(6), 853–63. doi:10.1002/jor.22002

Hermawan, H., Ramdan, D., & Djuansjah, J. R. P. (2009). Metals for Biomedical Applications. In R. Fazel (Ed.), *Biomedical Engineering - From Theory to Applications* (pp. 411–430). InTech. Retrieved from www.intechopen.com/download/get/type/pdfs/id/18658

Holy, C. E., Shoichet, M. S., & Davies, J. E. (2000). Engineering three-dimensional bone tissue in vitro using biodegradable scaffolds : Investigating initial cell-seeding density and culture period. *Journal of Biomedical Materials research*, *51*(3), 376–382.

Huiskes, R., Weinans, H., & van Rietbergen, B. (1992). The relationship between stress shielding and bone resorption around total hip stems and the effects of flexible materials. *Clinical orthopaedics and related research*, *274*, 124–134.

Karageorgiou, V., & Kaplan, D. (2005). Porosity of 3D biomaterial scaffolds and osteogenesis. *Biomaterials*, *26*(27), 5474–91. doi:10.1016/j.biomaterials.2005.02.002

Karsenty, G. (2007). Update on the transcriptional control of osteoblast differentiation. *BoneKEy-Osteovision*, *4*(6), 164–170. doi:10.1138/20070262

Kern, S., Eichler, H., Stoeve, J., Klüter, H., & Bieback, K. (2006). Comparative analysis of mesenchymal stem cells from bone marrow, umbilical cord blood, or adipose tissue. *Stem cells*, *24*(5), 1294–301. doi:10.1634/stemcells.2005-0342

Kerr, J. B. (2010). *Functional Histology* (2nd ed.). Melbourne, Australia: Mosby Elsevier Health Science.

Kierszenbaum, A. (2007). *Histology & Cell Biology: An introduction to pathology* (2nd ed.). Philadelphia, USA: Mosby Elsevier Health Science.

Komori, T. (2006). Regulation of osteoblast differentiation by transcriptional factors. *Journal of cellular biochemistry*, *99*, 1233–1239.

Kruse, P., & Patterson, M. (1973). *Tissue Culture methods and applications*. New York: Academic Press.

Kurtz, S., Ong, K., Lau, E., Mowat, F., & Halpern, M. (2007). Projections of primary and revision hip and knee arthroplasty in the United States from 2005 to 2030. *The Journal of bone and joint surgery. American volume*, *89*(4), 780–5. doi:10.2106/JBJS.F.00222

Lane, W. (1895). Some remarks on the treatment of fractures. *British medical journal*, *1*, 861.

Lavenus, S., Berreur, M., Trichet, V., Pilet, P., Louarn, G., & Layrolle, P. (2011). ADHESION AND OSTEOGENIC DIFFERENTIATION OF HUMAN MESENCHYMAL. *European Cells and Materials*, *22*, 84–96.

Le Guehennec, L., Lopez-Heredia, M.-A., Enkel, B., Weiss, P., Amouriq, Y., & Layrolle, P. (2008). Osteoblastic cell behaviour on different titanium implant surfaces. *Acta biomaterialia*, *4*(3), 535–43. doi:10.1016/j.actbio.2007.12.002

Le Guehennec, L., Soueidan, A., Layrolle, P., & Amouriq, Y. (2007). Surface treatments of titanium dental implants for rapid osseointegration. *Dental Materials Journal*, *23*, 844–854.

Li, J. P., Habibovic, P., van den Doel, M., Wilson, C. E., de Wijn, J. R., van Blitterswijk, C. a, & de Groot, K. (2007). Bone ingrowth in porous titanium implants produced by 3D fiber deposition. *Biomaterials*, *28*(18), 2810–20. doi:10.1016/j.biomaterials.2007.02.020

Loew, M. (2013). [Short stem shoulder prosthesis: Concept and first results]. *Der Orthopäde*, *42*(7), 501–506.

Maeda, M., Hirose, M., Ohgushi, H., & Kirita, T. (2007). In vitro Mineralization by Mesenchymal Stem Cells Cultured on Titanium Scaffolds. *The Journal of Biochemistry*, *736*, 729–736. doi:10.1093/jb/mvm077

Marion, N. W., & Mao, J. J. (2006). Mesenchymal stem cells and tissue engineering. *Methods in enzymology*, *420*(06), 339–61. doi:10.1016/S0076-6879(06)20016-8

Meinel, L., Karageorgiou, V., Fajardo, R., Snyder, B., Shinde-Patil, V., Zichner, L., … Vunjak-Novakovic, G. (2004). Bone tissue engineering using human mesenchymal stem cells: effects of scaffold material and medium flow. *Annals of biomedical engineering*, *32*(1), 112–22. Retrieved from http://www.ncbi.nlm.nih.gov/pubmed/14964727

Morris, H., Ochi, S., Spray, J., & Olson, J. (2000). Periodontal-type measurements associated with hydroxyapatite-coated and non-HA-coated implants: Uncovering to 36 months. *Annals of Periodontology*, *4*, 56–67.

Mudd, R., Vicatos, G., & Basson, J. (2003). *The charaterisation of the wear performance of thermally oxidised titanium surfacce and medical grade ultra high molecular weight polyethylene wear couples for orthopaedic applications*. University of Cape Town.

National Joint Registry. (2012). *National Joint Registry for England and Wales 9th Annual report*. (Martyn Porter, M. Borroff, P. Gregg, P. Howard, A. MacGregor, & K. Tucker, Eds.).

Nishiguchi, S, Kato, H., Fujita, H., Oka, M., Kim, H. M., Kokubo, T., & Nakamura, T. (2001). Titanium metals form direct bonding to bone after alkali and heat treatments. *Biomaterials*, *22*(18), 2525–2533. Retrieved from http://www.ncbi.nlm.nih.gov/entrez/query.fcgi?cmd=Retrieve&db=PubMed&dopt=Citation&list_uids=11516085

Nishiguchi, Shigeru, Fujibayashi, S., Kim, H.-M., Kokubo, T., & Nakamura, T. (2003). Biology of alkali- and heat-treated titanium implants. *Journal of biomedical materials research. Part A*, *67*(1), 26–35. doi:10.1002/jbm.a.10540

Okochi, H. (2011). Adult Stem Cells: Sources and Characterization. In N. Pallua & C. Suschek (Eds.), *Tissue engineering* (pp. 83–92). Berlin Heidelberg: Springer-Verlag. doi:10.1007/978-3-642-02824-3

Oreffo, R. O. C., & Triffitt, J. T. (1999). Future Potentials for Using Osteogenic Stem Cells and Biomaterials in Orthopedics. *Bone*, *25*(2), 5–9.

Orimo, H. (2010). The mechanism of mineralization and the role of alkaline phosphatase in health and disease. *Journal of Nippon Medical School*, *77*(1), 4–12.

Otsuki, B., Takemoto, M., Fujibayashi, S., Neo, M., Kokubo, T., & Nakamura, T. (2006). Pore throat size and connectivity determine bone and tissue

ingrowth into porous implants: three-dimensional micro-CT based structural analyses of porous bioactive titanium implants. *Biomaterials*, *27*(35), 5892–900. doi:10.1016/j.biomaterials.2006.08.013

Palmquist, A., Lindberg, F., Emanuelsson, L., Brånemark, R., Engqvist, H., & Thomsen, P. (2009). Morphological studies on machined implants of commercially pure titanium and titanium alloy (Ti6Al4V) in the rabbit. *Journal of biomedical materials research. Part B, Applied biomaterials*, *91*(1), 309–19. doi:10.1002/jbm.b.31404

Panagis, J., Saled, K., & Sledge, C. (2013). Questions and answers about Hip replacements. *National institute of arthritis and musculoskeletal and skin diseases*. Retrieved January 31, 2014, from http://www.niams.nih.gov/health_info/Hip_Replacement/default.asp

Pearsons Education Inc. (2006). Stages of Intramembranous Ossification. Retrieved January 12, 2014, from http://www.kean.edu/~jfasick/docs/Fall Semester Lectures Chapt. 1-15 '07/Chapter 6B.pdf

Pederson, R. (2002). *Microstructure and Phase Transformation of Ti-6Al-4V*. Lulea University of Technology.

Peltola, S. M., Grijpma, D. W., Melchels, F. P. W., & Kelomaki, M. (2008). A review of rapid prototyping techniques for tissue engineering purposes. *Annals of Medicine*, *40*(4), 268–280.

Perren, S., Geret, V., Tepic, M., & Rahn, B. (1986). Quantitative evaluation of biocompatibility of vanadium free titanium alloys. In L. Christel, A. Meunier, & A. Lee (Eds.), *Biological and biomechanical performance of biomaterials* (pp. 397–402). Amsterdam: Elsevier Science.

Perrotti, V., Palmieri, A., Pellati, A., Degidi, M., Ricci, L., Piattelli, A., & Carinci, F. (2013). Effect of titanium surface topographies on human bone marrow stem cells differentiation in vitro. *Odontology*, *101*(2), 133–139. doi:10.1007/s10266-012-0067-0

Pfister, A., Landers, D., Laib, A., Hubner, U., Schmelzeisen, R., & Mulhaupt, R. (2003). Biofunctional Rapid Prototyping for Tissue-Engineering Applications : 3D Bioplotting versus 3D Printing *. *Journal of Polymer Science: Part A: Polymer Chemistry*, *42*, 624–638.

Pohler, O. E. M. (2000). Unalloyed titanium for implants in bone surgery. *Injury*, *31*(4), 7–13.

Poli, C. (2001). *Design for Manufacturing: A structured approach, Volume 1* (1st ed.). Woburn, MA: Butterworth-Heinemann.

Porter, M, Borroff, M., Gregg, P., Howard, P., MacGregor, A., & Tucker, K. (2012). *National Joint Registry for England and Wales 9th Annual report* (Vol. 50).

Ratner, B., Hoffman, A., Schoen, F., & Lemons, J. (2012). A History of Biomaterials. In *Biomaterials Science: An introdction to materials in medicine* (3rd ed.). Academic Press.

Ross, M., & Pawlina, W. (2011). *Histology: A text & atlas* (6th ed.). Philadelphia, USA: Lippincott Williams & Wilkins.

Rothman, R., & Cohn, J. (1990). Cemented versus cementless total hip arthroplasty. A clinical review. *Clinical orthopaedics and related research*, *254*, 153–169.

Sakaguchi, Y., Sekiya, I., Yagishita, K., & Muneta, T. (2005). Comparison of human stem cells derived from various mesenchymal tissues: superiority of synovium as a cell source. *Arthritis and rheumatism*, *52*(8), 2521–9. doi:10.1002/art.21212

Saldaña, L., Vilaboa, N., Vallés, G., González-Cabrero, J., & Munuera, L. (2005). Osteoblast response to thermally oxidized Ti6Al4V alloy. *Journal of biomedical materials research. Part A*, *73*(1), 97–107. doi:10.1002/jbm.a.30264

Schindler, P. (1984). Surface complexation. In H. Sigel (Ed.), *Metal ions in biological systems* (23rd ed., pp. 105–135). New York: Dekker.

Smith, S. M., & Heer, M. (2002). Calcium and bone metabolism during space flight. *Nutrition*, *18*(10), 849–52. Retrieved from http://www.ncbi.nlm.nih.gov/pubmed/15647814

Sobral, J. M., Caridade, S. G., Sousa, R. a, Mano, J. F., & Reis, R. L. (2011). Three-dimensional plotted scaffolds with controlled pore size gradients: Effect of scaffold geometry on mechanical performance and cell seeding efficiency. *Acta biomaterialia*, *7*(3), 1009–18. doi:10.1016/j.actbio.2010.11.003

Sotiropoulou, P. a, Perez, S. a, Salagianni, M., Baxevanis, C. N., & Papamichail, M. (2006). Characterization of the optimal culture conditions for clinical scale production of human mesenchymal stem cells. *Stem cells*, *24*(2), 462–71. doi:10.1634/stemcells.2004-0331

Steinemann, G. (1998). Titanium - the material of choice ? *Periodontology 2000*, *17*, 7–21.

Stenderup, K., Justesen, J., Clausen, C., & Kassem, M. (2003). Aging is associated with decreased maximal life span and accelerated senescence of bone marrow stromal cells. *Bone*, *33*, 919–926. doi:10.1016/j.bone.2003.07.005

Stiehler, M., Lind, M., Mygind, T., Baatrup, A., Dolatshahi-pirouz, A., Li, H., … Bu, C. (2008). Morphology , proliferation , and osteogenic differentiation of mesenchymal stem cells cultured on titanium , tantalum , and chromium surfaces. *Journal of Biomedical Materials research Part A*, *86A*(2), 448–458. doi:10.1002/jbm.a.31602

St-Pierre, J.-P., Gauthier, M., Lefebvre, L.-P., & Tabrizian, M. (2005). Three-dimensional growth of differentiating MC3T3-E1 pre-osteoblasts on porous titanium scaffolds. *Biomaterials*, *26*(35), 7319–28. doi:10.1016/j.biomaterials.2005.05.046

Takemoto, M., Fujibayashi, S., Neo, M., Suzuki, J., Kokubo, T., & Nakamura, T. (2005). Mechanical properties and osteoconductivity of porous bioactive titanium. *Biomaterials*, *26*(30), 6014–23. doi:10.1016/j.biomaterials.2005.03.019

Thermo Fisher Scientific Inc., & Kamath, A. (2009). Human Mesenchymal Stem Cells and Multipotent Cord Blood Unrestricted Somatic Stem Cell Protocol : Thawing and Plating. Retrieved from http://www.thermoscientific.fr/eThermo/CMA/PDFs/Various/File_4338.pdf

Turner, C. H. (1998). Three Rules for Bone Adaptation to Mechanical Stimuli. *Bone*, *23*(5), 399–407.

Waddell, J. (2008). *Hip arthritis surgery* (1st ed.). Philadelphia, USA: Saunders, Elsevier Inc.

Waterhouse, R. B., & Iwabuchi, A. (1985). High temperatures fretting wear of four titanium alloys. *Wear*, *106*, 303–313.

Waters, M., Gardner, D., & Coffin, D. (1974). Cytotoxic effects of vanadium on rabbit alveolar macrophages in vitro. *Toxicology and applied pharmacology*, *28*(2), 253–263.

Wennerberg, A., Albrektsson, T., Albrektsson, B., & Krol, J. (1995). Histomorphometric and removal torque study of screw-shaped titanium

implants with three different surface topographies. *Clinical oral implants research*, *6*, 24–30.

Wilkinson, J., Gordon, A., & Stockley, I. (2003). Experiences with the Plasmacup - early stability, wear, remodelling and outcome. *International Orthopaedics*, *27 Suppl 1*, S16–9.

Yang, Y., Tian, J., Deng, L., & Ong, J. L. (2002). Morphological behavior of osteoblast-like cells on surface-modified titanium in vitro. *Biomaterials*, *23*, 1383–1389.

Zhao, R. (2013). *Essentials of mesenchymal stem cell biology and its clinical translation*. (R. Zhao, Ed.). Dordrecht: Springer Science+ Business Media.

Appendix A. Tissue culture medium Recipes

Standard Culture Medium (for rat MSCs)

88% Dulbecco's modified Eagle medium (DMEM) (Gibco 52100-021)

10% Foetal bovine serum (FBS) (PAA)

2% Penicillin/Steptomycin (final concentrations of 100 U/ml for each)

Standard Culture Medium (for human MSCs)

88% alpha Minimum essentials medium (αMEM) (Gibco 32561-029)

10% FBS (PAA)

2% Penicillin/Steptomycin (final concentrations of 100 U/ml for each)

Freeze Medium 2X concentration

20% Dimethyl sulfoxide (DMSO)

60% FBS (PAA)

20% αMEM (Gibco 32561-029)

Osteogenic Medium

88% DMEM (Gibco 52100-021)

10% FBS (PAA)

1% Penicillin/Steptomycin (final concentrations of 100 U/ml for each)

For every 250 ml medium add the following osteogenic factors:

0.004 g Ascorbic -2- phosphate (Sigma 49752)

0.765 g β-glycerophosphate (Sigma 50020)

1 ml 0.01% Dexamethasone (Sigma D4902)

Stir solution for 1 hour and filter

Phosphate Buffer Solution (PBS) 1X concentration

For one litre solution, combine:

8 g Sodium chloride (NaCl)

1.26 g Sodium phosphate (Na_2HPO_4)

0.2 g Potassium chloride (KCl)

0.2 g Potassium phosphate (KH_2PO_4)

Dissolve in and make up to 1 litre with double distilled water

pH to 7.4

Hoechst LIVE stain medium

For every 10 ml medium, combine:

40 µl Hoechst 33342 fluorescent stain (Invitrogen H1399)

9.96 ml PBS

Alizarin Red LIVE stain medium

For every 50 ml medium, combine:

25 µg Alizarin red S powder (Sigma A5533)

50 ml Standard culture medium

Appendix B. Tissue culture Protocols

Appendix B.1: Thawing of MSCs

1. Pipette in 8 ml Standard culture medium (see **Standard culture medium recipe**) into 15 ml tube and warm in waterbath
2. Remove cells from liquid nitrogen stocks and place in ethanol swab
3. Swab cryovial with ethanol to disinfect
4. Pipette warmed medium into cryovial and immediately transfer thawing cells into 15 ml tube
5. Repeat until entire cyrovial contents have been transferred into 15 ml tube
6. Centrifuge cells at 1000 rpm for 3 minutes
7. Suction off supernatant and resuspend to a density of ±5,000 cells/cm^2 in Standard culture medium
    a. 4.5-5x10^4 cells in 10 ml in 10 cm dish
    b. 1.25-1.5x10^5 cells in 5 ml in T25 flask
    c. 3.75-4x10^5 cells in 7 ml in T75 flask
8. Incubate. Check cells under light microscope to determine whether a complete medium change is necessary 24 hours later
9. Maintain cells following Maintenance Protocol

Appendix B.2: Maintenance of MSCs in Standard culture medium

1. Two days after initial seeding, and on a Wednesday, half the medium was pipette off cells and replenished with equal volume Standard culture medium (see **Standard culture medium recipe**)
    a. 5 ml in 10 cm dish
    b. 2.5 ml in T25 flask
    c. 3.5 ml in T75 flask
2. On a Monday and Friday all the medium was suctioned off cells and replenished with full volume of Standard culture medium
    a. 10 ml in 10 cm dish
    b. 5 ml in T25 flask

   c. 7 ml in T75 flask
3. Passage when cells reach 80-90% confluency following Passaging Protocol

Appendix B.3: Passaging of MSCs

1. Suction off medium and rinse twice with 5 ml PBS (see **PBS 1X concentration recipe**) and remove
2. Pipette 1X trypsin/EDTA onto cells and incubate for 5 minutes
   a. 1 ml for 10 cm dish
   b. 1 ml for T25 flask
   c. 3 ml for T75 flask
3. Tap dish/flask to loosen cells
4. Pipette equal volume of Standard culture medium (see **Standard culture medium recipe**) onto cells to inactivate and triturate gently and further loosen and wash cells from flask.
5. Transfer cell suspension to 15 ml tube
6. Rewash flask with medium and transfer to same 15 ml tube to collect any remaining cells
   a. 2 ml for 10 cm dish
   b. 2 ml for T25 flask
   c. 5 ml for T75 flask
7. Centrifuge cells at 1000 rpm for 3 minutes
8. Suction off supernatant and resuspend cells in 1 ml of Standard culture medium. Triturate to ensure single cell suspension in solution.
9. Pipette 7 ul onto haemocytometer and count cells if necessary
10. Plate at ±5,000 cells/cm^2 in Standard culture medium
    a. 1.25-1.5x10^5 cells in 5 ml in T25 flask
    b. 3.75-4x10^5 cells in 7 ml in T75 flask
11. Maintain cells following Maintenance Protocol

Appendix B.4: Osteogenic differentiation of MSCs

1. Passage cells using steps 1-9 of Passaging Protocol
2. Resuspend cells to a density of ±10,000 cells/cm^2 in Standard culture medium (see **Standard culture medium recipe**)
    a. $9.5x10^4$ cells in 2 ml in each well of 6 well plate
    b. $5.5x10^5$ cells in 10 ml in 10 cm dish
3. Incubate for 48 hours (confirm confluency by phase contrast microscopy to be 50-80%)
4. Suction off Standard culture medium and pipette on equal volume Osteogenic medium (see **Osteogenic medium recipe**)
5. On a Monday and Friday, all medium was suctioned off and replenished with equal volume Osteogenic medium.

Appendix B.5: Freezing of MSCs

1. Passage cells using steps 1-9 of Passaging Protocol
2. Centrifuge cells at 1000 rpm for 3 minutes
3. Suction off supernatant and resuspend cells in Standard culture medium (see **Standard culture medium recipe**) to a concentration of $2x10^6$ cells/ml
4. Label enough cryovials and tranfer 0.5 ml of cell suspension into each
5. Add 0.5 ml of 2X Freeze medium (see **Freeze medium 2X concentration recipe**) into each cryovial and trituate once gently to mix
6. Immediately place cryovial on ice and then into -80 °C freezer overnight
7. 24 hours later transfer cryovials to liquid nitrogen tanks for long term storage

Appendix B.6: Staining osteogenic differentiation

1. Suction off all medium and rinse twice with 2 ml PBS (see **PBS 1X concentration recipe**) and remove
2. Pipette Alizarin red LIVE stain medium (see **Alizarin red LIVE stain medium recipe**) onto cells
    a. 2 ml per well of 6 well plate

   b. 5 ml in 10 cm dish
3. Incubate for 1 hour
4. Suction off Alizarin red LIVE stain medium (see **Alizarin red LIVE stain medium recipe**) and rinse twice with 2 ml PBS and remove
5. Pipette Hoechst LIVE stain (see **Hoechst LIVE stain medium recipe**) onto cells and incubate
   a. 2 ml per well of 6 well plate
   b. 5 ml in 10 cm dish
6. After 10-15 minutes, view under fluorescence microscope.

Appendix C: Ti64 scaffold tissue culture protocols

Appendix C.1: Seeding MSCs on Ti64 scaffolds

1. Passage cells from dish/flask following Passaging Protocol (steps 1-9)
2. Centrifuge cells at 1000 rpm for 3 minutes
3. Resuspend cells in Standard culture medium (see **Standard culture medium recipe**) taking into account final seed efficiency, scaffold size, required seeding volume and number of scaffolds to seed in order to obtain a final seed of 5,000 cells/cm2 for growth experiment or 10,000 cells/cm2 for differentiation experiment
    a. rMSCs have a 40% seeding efficiency, thus for growth experiments:
        i. $15x10^4$ cells in 0.4 ml per 11.17 cm^2 scaffold
        ii. $11.5x10^4$ cells in 0.3 ml per 8.29 cm^2 scaffold
    b. rMSCs have a 40% seeding efficiency, thus for differentiation experiments:
        i. $30x10^4$ cells in 0.4 ml per 11.17 cm^2 scaffold
        ii. $23x10^4$ cells in 0.3 ml per 8.29 cm^2 scaffold
    c. hMSCs have a 20% seeding efficiency, thus for growth experiments:
        i. $28x10^4$ cells in 0.4 ml per 11.17 cm^2 scaffold
        ii. $21x10^4$ cells in 0.3 ml per 8.29 cm^2 scaffold
    d. hMSCs have a 20% seeding efficiency, thus for differentiation experiments:
        i. $56x10^4$ cells in 0.4 ml per 11.17 cm^2 scaffold
        ii. $42x10^4$ cells in 0.3 ml per 8.29 cm^2 scaffold
4. Place scaffolds into tissue culture plates for seeding
    a. 11.17 cm^2 scaffolds into 6 well plates
    b. 8.29 cm^2 scaffolds into 12 well plates
5. Pipette the cell suspension onto the top of the scaffold surface of the Ti64 disk to form a meniscus. Be careful not to allow liquid to spill over sides of disk
    a. 0.4 ml onto 11.17 cm^2 scaffolds
    b. 0.3 ml onto 8.29 cm^2 scaffolds
6. Incubate, being careful not to disturb meniscus.

7. After one hour, flood scaffolds with Standard culture medium (see **Standard culture medium recipe**) until submerged
    a. Add 2.6 ml to 11.17 cm^2 scaffolds
    b. Add 0.7 ml to 8.29 cm^2 scaffolds
8. Maintain cells following Maintenance on Ti64 Protocol

Appendix C.2: Maintenance on Ti64 of MSCs in Standard culture medium

1. Two days after initial seeding, and on a Wednesday, half the medium was pipette off scaffolds and replenished with equal volume Standard culture medium (see **Standard culture medium recipe**)
    a. 1.5 ml on 11.17 cm^2 scaffolds
    b. 0.5 ml on 8.29 cm^2 scaffolds
2. On a Monday and Friday all the medium was suctioned off scaffolds and replenished with full volume of Standard culture medium
    a. 3 ml on 11.17 cm^2 scaffolds
    b. 1 ml on 8.29 cm^2 scaffolds

Appendix C.3: Osteogenic Differentiation maintenance on Ti64

1. Seed scaffolds following Seeding Ti64 Protocol
2. Two days after seeding, and on Mondays and Fridays all medium is suctioned off scaffolds and replenished with equal volume Osteogenic medium (see **Osteogenic medium recipe**)
    a. 3 ml on 11.17 cm^2 scaffolds
    b. 1 ml on 8.29 cm^2 scaffolds

Appendix C.4: Passaging MSCs on Ti64 scaffolds

1. Suction off medium and rinse twice with 2 ml PBS (see **PBS 1X concentration recipe**) and remove
2. Transfer scaffold to a new plate
    a. 11.17 cm^2 in 6 well plate
    b. 8.29 cm^2 in 12 well plate
3. Pipette 1X trypsin/EDTA onto scaffolds and incubate for 5 minutes
    a. 2 ml onto 11.17 cm^2 scaffolds
    b. 1 ml for 8.29 cm^2 scaffolds
4. Pipette equal volume of Standard culture medium (see **Standard culture medium recipe**) onto cells to inactivate and triturate gently and further loosen and wash cells from flask.
5. Using forceps, hold scaffold vertically and pipette medium through scaffold left to right 3-4 times (medium will run our bottom of scaffold back into dish).
6. Still holding scaffold, pipette medium through scaffold top to bottom 3-4 times
7. Rotate scaffold 90°, keeping it vertical, and repeat steps 5 and 6.
8. Transfer cell suspension to 15 ml tube
9. Pipette 2 ml fresh Standard culture medium onto scaffold (either size). Repeat steps 5-8 with fresh medium.
10. Centrifuge cells at 1000 rpm for 3 minutes
11. Suction off supernatant and resuspend cells in 0.5 ml of Standard culture medium. Triturate to ensure single cell suspension in solution.
12. Pipette 7 ul onto haemocytometer and count cells

Appendix C.5: Staining osteogenic differentiation on Ti64 scaffolds

1. Suction off all medium and rinse twice with 2 ml PBS (see **PBS 1X concentration recipe**) and remove
2. Pipette Alizarin red LIVE stain medium (see **Alizarin red LIVE stain medium recipe**) onto scaffolds
    a. 2 ml onto 11.17 cm^2 scaffolds

   b. 1 ml for 8.29 cm^2 scaffolds
3. Incubate for 1 hour
4. Suction off Alizarin red LIVE stain medium and rinse twice with 2 ml PBS and remove
5. Pipette Hoechst LIVE stain (see **Hoechst LIVE stain medium recipe**) onto cells and incubate
   a. 2 ml onto 11.17 cm^2 scaffolds
   b. 1 ml for 8.29 cm^2 scaffolds
6. After 10-15 minutes, invert scaffold in medium and view under fluorescence microscope.